of plasma ir-uroguanylin. However, uroguanylin mRNA in the intestine never increased, indicating that uroguanylin acts in the kidney as an autocrine and/or paracrine factor.

Uroguanylin probably participates in regulation of the sodium balance in the kidney. However, the natriuretic effects of uroguanylin as a therapeutic agent under sodium and water retention have not been investigated. This study evaluates whether exogenous uroguanylin administration induces natriuresis during the period of sodium retention in rats with PAN-induced nephrosis.

METHODS

Animals and peptide

Male Sprague–Dawley rats (Charles River, Kanagawa, Japan) weighing 160–230 g were housed in a temperature and light-controlled environment with a 12:12 h light : dark cycle and placed in individual metabolic cages 1 day before starting experiments. Nephrotic rats were allowed free access to standard rat chow (Nihon CLEA, Tokyo, Japan) and water throughout the study, whereas pair-fed control animals had free access to water but received the mean daily intake of the corresponding nephrotic rats. Rat uroguanylin was provided by the Peptide Institute (Osaka, Japan).

Experimental protocol

In study 1, the rats were randomized into four groups as follows: untreated controls (group I, $n = 6$); uroguanylin-treated controls (group II, $n = 6$); untreated nephrotic rats (group III, $n = 10$); and uroguanylin-treated nephrotic rats (group IV, $n = 10$). Nephrosis was induced by a single i.p. injection of 150 mg/kg of PAN (Sigma, St Louis, MO, USA) dissolved in saline (day 0). Control groups were injected with an equivalent volume of saline.

On day 4, the treated rats were anaesthetized with pentobarbital sodium, and i.p. implanted with micro-osmotic pumps (model 1003D; Durect, Cupertino, CA, USA) that were scheduled to release 0.5 nmol/h of rat uroguanylin in water over 3 days. The untreated groups were similarly infused with vehicle. The timing of uroguanylin administration was matched to the sodium retention phase[15] when uroguanylin excretion peaks and is followed by natriuresis in nephrotic rats. The dose of uroguanylin was adjusted to produce an equivalent peak in normal rats to that expected in nephrotic rats.

Urinary sodium, protein, creatinine, ir-uroguanylin and cyclic guanylic acid (cGMP) were measured in 24 h urine samples. Urinary sodium, protein and creatinine were measured by indirect potentiometry using an automatic analyzer with ion-selective electrodes, by colourimetric reactions using pyrogallol red and by the enzymatic assay, respectively.

In study 2, 48 rats ($n = 6$/group × four groups × two sets) were treated in the same way as in study 1 and then killed for blood and tissue sampling on days 6 and 12. Blood was collected into chilled polypropylene tubes containing ethylenediaminetetraacetic acid (EDTA)-2Na (1 mg/mL blood) and aprotinin (500 units/mL blood), then immediately centrifuged at 1700 *g* for 15 min at 4°C. The kidneys and upper small intestines were resected and frozen for RNA extraction and cGMP assays. Differences in the circadian expression of uroguanylin were avoided by standardizing the experimental schedule for both groups.

All experiments described above proceeded according to the regulations established by the Animal Research Committee of Miyazaki University.

Uroguanylin and cGMP assays

The uroguanylin radioimmunoassay (RIA) for plasma and urine proceeded as described by Fukae *et al.*[8] This RIA specifically recognizes uroguanylin and prouroguanylin, both of which contain reduced and S-carboxymethylated (RCM) forms.

Tissues and urinary cGMP concentrations were determined using a cGMP enzyme-linked immunosorbent assay (ELISA). Samples were homogenized or precipitated with 6% trichloroacetic acid (TCA) on ice. The supernatant was washed with water-saturated diethyl ether to remove the TCA. The residue was evaporated to dryness, reconstituted in assay buffer and measured using an ELISA kit (GE Healthcare, Buckinghamshire, UK).

Real-time reverse transcriptase-polymerase chain reaction

Total RNA (5 μg) extracted using the total RNA Isolation Reagent (Invitrogen, Carlsbad, CA, USA) was reverse-transcribed using Superscript Reverse Transcriptase (Invitrogen) into cDNA. Rat uroguanylin mRNA levels were measured by Real-Time Quantitative PCR (ABI Prism 7700 Sequence Detector; Applied Biosystems, Foster City, CA, USA) as described.[15] The cDNA was amplified using forward and reverse oligonucleotide primers, and probes were quenched with 6-carboxytetramethyl-rhodamine. Levels of uroguanylin mRNA were normalized to those of internal control glyceraldehyde 3-phosphate dehydrogenase (GAPDH) mRNA. All polymerase chain reaction (PCR) products were verified once by sequencing and all reactions proceeded in duplicate.

Statistical analysis

All data are presented as means ± standard error of the mean. We applied the one-way ANOVA to compare parametric data among the four groups. Significances of individual differences were evaluated by using the Tukey–Kramer test if the ANOVA findings were significant. $P < 0.05$ was considered statistically significant in all calculations.

RESULTS

In study 1, PAN-induced nephrosis affected urinary sodium excretion and urinary ir-uroguanylin excretion (Fig. 1). The urinary sodium excretion was decreased during the early phase (sodium retention) and increased later (natriuretic phase) in nephrotic rats. Urinary ir-uroguanylin excretion was increased in nephrotic compared with control rats without uroguanylin administration on days 9–12.

Uroguanylin did not increase urinary sodium excretion in control rats (Fig. 2a). On the other hand, exogenous uroguanylin increased urinary sodium excretion in the nephrotic groups on days 6–8 (Fig. 2b; group III vs group IV in mmol/mmol creatinine; 2.92 ± 0.65 vs 8.93 ± 2.53 on day 6, $P < 0.05$; 3.55 ± 0.47 vs 10.37 ± 1.73 on day 7, $P < 0.01$; and 14.88 ± 2.32 vs 24.47 ± 2.86 on day 8, $P < 0.05$).

The urinary excretion of ir-uroguanylin during uroguanylin administration was obviously increased in groups II and IV, and the peak of ir-uroguanylin in normal rats (group II) was comparable with the natriuretic phase of nephrotic rats (group III) (Fig. 3).

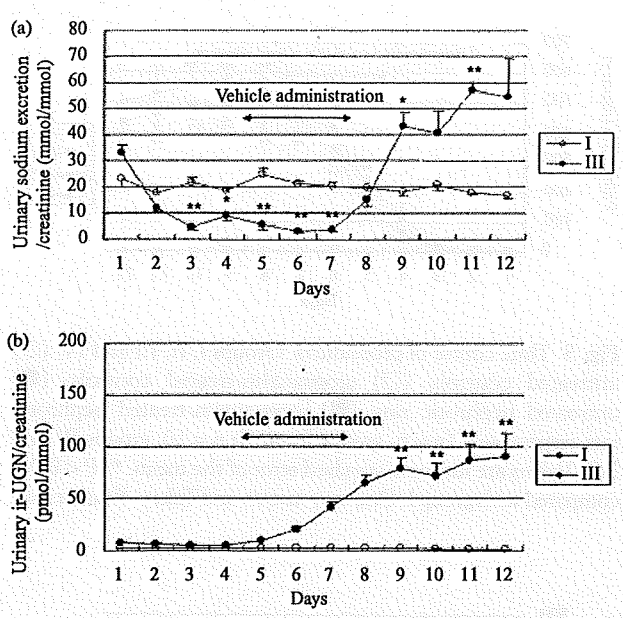

Fig. 1 Time course of urinary sodium excretion (a) and immunoreactive-uroguanylin (ir-UGN) (b) in normal and nephrotic rats without exogenous uroguanylin. Group I, untreated control rats. (○) $n = 6$. Group III, untreated nephrotic rats. (●) $n = 10$. Values are means ± standard error of the mean. $^*P < 0.05$; $^{**}P < 0.01$; compared with group I. One-way ANOVA and Tukey–Kramer test.

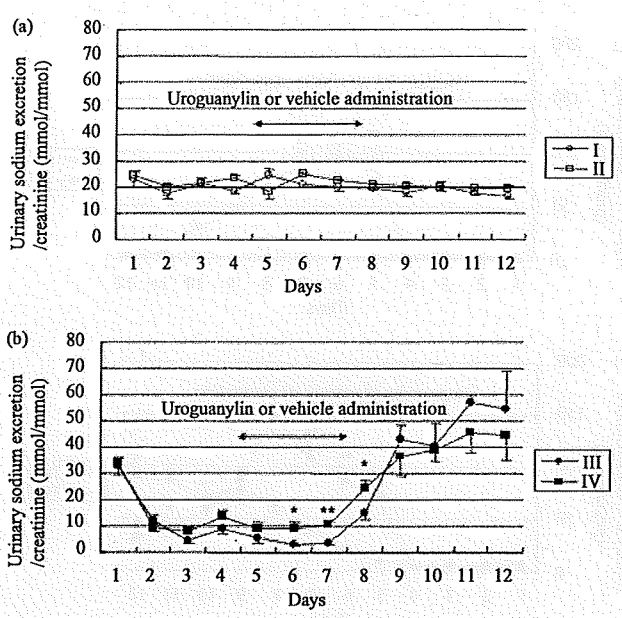

Fig. 2 Time course of urinary sodium excretion in control (a) and nephrotic (b) groups. Groups I, II, III and IV: (○) untreated controls; (□) uroguanylin-treated controls; (●) untreated nephrotic rats; and (■) uroguanylin-treated nephrotic rats respectively ($n = 6$, groups I and II; $n = 10$, groups III and IV). Values are means ± standard error of the mean (SEM). $^*P < 0.05$; $^{**}P < 0.01$; compared with group I (a) or group III (b). One-way ANOVA and Tukey–Kramer test.

Urine volume was significantly increased in the nephrotic rats (group III) compared with the control (phase of natriuresis) rats on days 8–11 (Fig. 4). However, exogenously administrated uroguanylin did not potentiate diuresis in the nephrotic groups (group III vs IV; Fig. 4). Both nephrotic groups developed proteinuria (Fig. 5), but exogenous uroguanylin did not alter the level of proteinuria in the nephrotic rats (group III vs IV, 453 ± 36.4 vs 444 ± 48.3 mg/day, on day 7). Urinary excretion of cGMP, the second messenger of uroguanylin, was decreased in the nephrotic rats compared with normal rats (Fig. 6), but this was not increased in uroguanylin-treated or untreated groups.

In study 2, Figure 7 compares the plasma concentration of ir-uroguanylin among the four groups. Uroguanylin administration increased the plasma level of ir-uroguanylin in control rats on day 6 (group I vs II), but the difference did not reach significance. The plasma level of ir-uroguanylin in nephrotic rats was increased in group IV compared with group III (group III vs group IV, 3.4 ± 0.6 vs 7.0 ± 0.7 pmol/mL, $P < 0.01$). The plasma ir-uroguanylin concentrations were similar in groups II and III. At day 12, plasma ir-uroguanylin levels did not differ among the four groups.

Nephrosis induction and/or uroguanylin administration did not increase tissue cGMP concentrations (groups I, II, III and IV: 15.31 ± 1.18, 20.67 ± 5.54, 25.33 ± 1.95 and 17.70 ± 3.94 fmol/mg tissue weight, respectively).

Uroguanylin mRNA expression in the kidneys on day 6 was decreased in nephrotic groups on day 6 (group I vs III: 100 ± 13.3 vs 49.5 ± 10.0%, $P < 0.05$ respectively) (Fig. 8a), and was unaffected by uroguanylin administration in nephrotic rats. On the other hand, expression levels in the intestines did not differ among the four groups (groups I, II, III and IV: 100 ± 19.3%, 120.0 ± 3.9%, 106.4 ± 18.8% and 97.7 ± 8.8%) (Fig. 8b).

DISCUSSION

Uroguanylin induces natriuresis in the isolated perfused kidney[4] and *in vivo*.[5,6] We previously found that urinary sodium excretion abruptly increases immediately after the period of retention in nephrotic syndrome, in accordance with increased urinary uroguanylin excretion.[15] However, whether exogenous uroguanylin elicits an increase in urinary sodium under pathological conditions with sodium retention remains unclear. The present study discovered that continuous, i.p. administration of uroguanylin induced increased sodium excretion into the urine during the period of sodium retention in nephrotic rats. Sodium and water retention comprise a major clinical problem in the management of patients with nephrotic syndrome, in which natriuresis by loop diuresis or atrial natriuretic peptide (ANP) is obviously attenuated.[16–18] Although further studies are

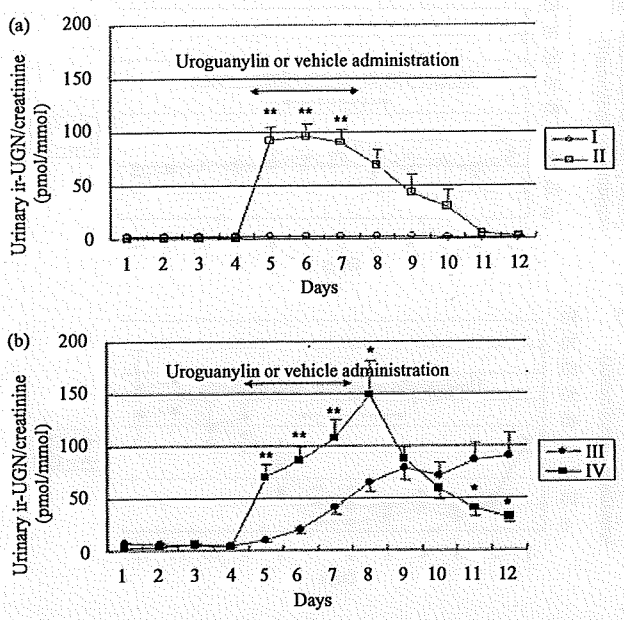

Fig. 3 Time course of urinary immunoreactive-uroguanylin (ir-UGN) excretion in control (a) and in nephrotic (b) rats. Groups I, II, III and IV: (○) untreated controls; (□) uroguanylin-treated controls; (●) untreated nephrotic rats; (■) uroguanylin-treated nephrotic rats respectively ($n = 6$, groups I and II; $n = 10$, groups III and IV). Values are means ± standard error of the mean. $^{*}P < 0.05$; $^{**}P < 0.01$; compared with group I (a) or group III (b). One-way ANOVA and Tukey–Kramer test.

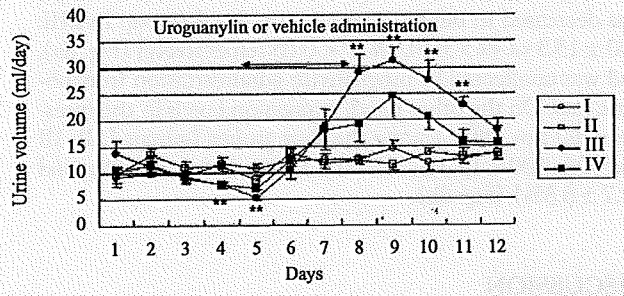

Fig. 4 Time course of urine volume. Groups I, II, III and IV: (○) untreated controls; (□) uroguanylin-treated controls; (●) untreated nephrotic rats; (■) uroguanylin-treated nephrotic rats respectively ($n = 6$, groups I and II; $n = 10$, groups III and IV). Values are means ± standard error of the mean. $^{**}P < 0.01$, compared with group I. One-way ANOVA and Tukey–Kramer test.

needed to verify the notion, uroguanylin might improve natriuretic activity in patients with nephrotic syndrome.

Uroguanylin did not promote sodium excretion in normal rats at the same dose as that administrated to nephrotic rats. The dose of uroguanylin administration in this study was lower than that of previous studies,[4–6] and might be insufficient to induce natriuresis. The plasma ir-uroguanylin concentration on day 6 was significantly

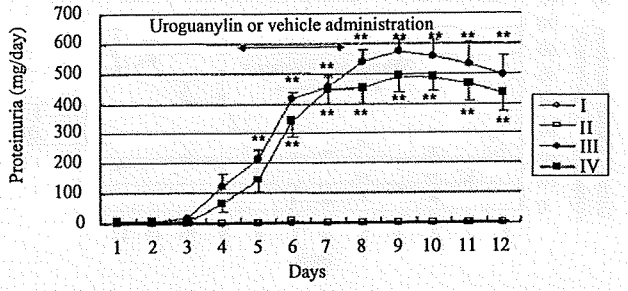

Fig. 5 Time course of proteinuria. Groups I, II, III and IV: (○) untreated controls; (□) uroguanylin-treated controls; (●) untreated nephrotic rats; (■) uroguanylin-treated nephrotic rats respectively ($n = 6$, groups I and II; $n = 10$, groups III and IV). Values are means ± standard error of the mean. $^{**}P < 0.01$, compared with group I. One-way ANOVA and Tukey–Kramer test.

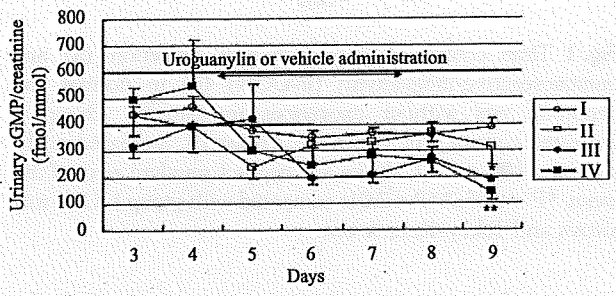

Fig. 6 Urinary cyclic 3′,5′-guanosine monophosphate (cGMP) excretion. Groups I, II, III and IV: (○) untreated controls; (□) uroguanylin-treated controls; (●) untreated nephrotic rats; (■) uroguanylin-treated nephrotic rats respectively ($n = 4$). Values are means ± standard error of the mean. $^{*}P < 0.05$; $^{**}P < 0.01$; compared with group I. One-way ANOVA and Tukey–Kramer test.

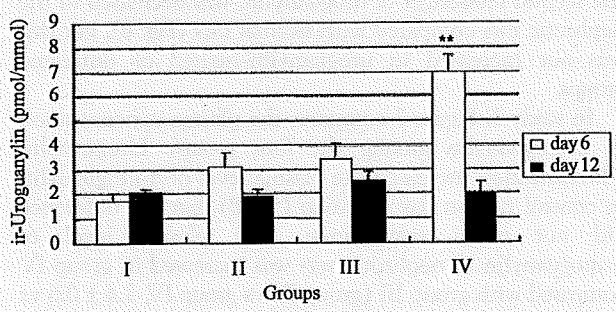

Fig. 7 Plasma concentration of immunoreactive (ir)-uroguanylin on days 6 (□) and 12 (■). Groups I, II III and IV: untreated controls, uroguanylin-treated controls, untreated nephrotic and uroguanylin-treated nephrotic rats respectively ($n = 6$). Values are means ± standard error of the mean. $^{**}P < 0.01$ compared with other groups. One-way ANOVA and Tukey–Kramer test.

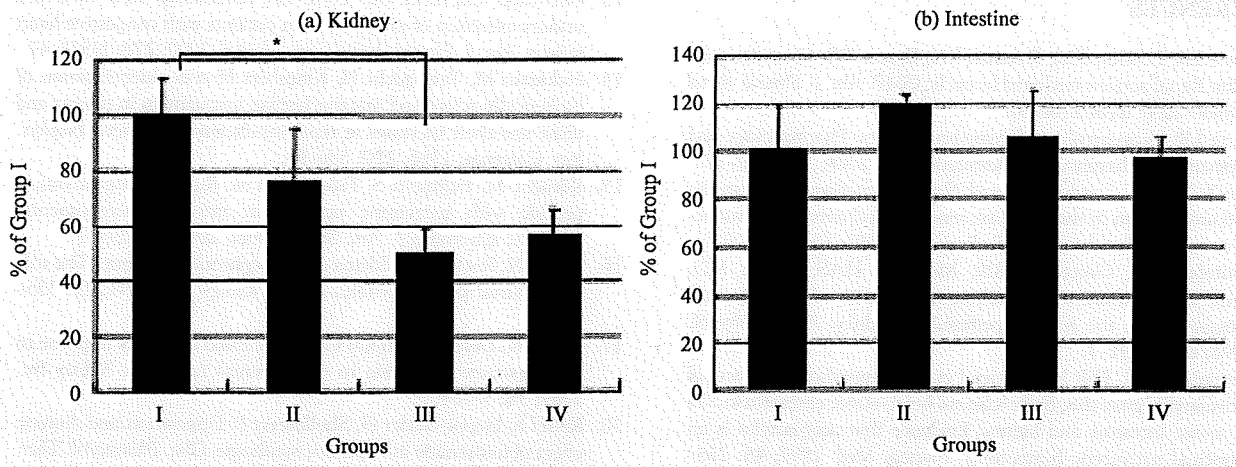

Fig. 8 Comparison in renal (a) and intestinal (b) uroguanylin mRNA expression on day 6. Groups I, II, III and IV: untreated controls, uroguanylin-treated controls, untreated nephrotic and uroguanylin-treated nephrotic rats, respectively ($n = 6$). Values are means ± standard error of the mean. *$P < 0.05$ compared with group I. One-way ANOVA and Tukey–Kramer test.

increased only in uroguanylin-treated nephrotic rats (Fig. 7), in which natriuresis was significant (Fig. 2). Additionally, sodium excretion was significantly suppressed during the sodium retention phase (Fig. 1) in nephrotic rats, and uroguanylin administration partially reversed this suppression, but the value did not increase to the normal range in nephrotic rats (Fig. 2). The status of the sodium balance could influence the sensitivity of the kidney to uroguanylin. However, further studies are required to clarify this notion.

Increased production and/or a decrease in uroguanylin metabolism would be required to increase the plasma ir-uroguanylin concentration in nephrosis. However, the level of uroguanylin mRNA in the intestine was not changed among the four groups and that in the kidney had not increased in nephrotic rats on day 6 (Fig. 8). These results suggested that uroguanylin production does not always increase in nephrosis. The excretion of exogenously administrated uroguanylin into the urine persisted for 3 days after termination (Fig. 3), so uroguanylin might be retained for longer in plasma, thus generating a time-lag between uroguanylin production and accumulation. Furthermore, metabolism might be different in nephrosis. We previously showed by reverse-phase high-performance liquid chromatography coupled with RIA that urinary ir-uroguanylin has two major immunoreactive peaks in nephrotic rats.[15] The main form was bioactive uroguanylin and the remainder was a precursor, whereas normal urine has only the bioactive peak. In addition, the plasma and urinary uroguanylin precursor concentration is increased in patients with chronic glomerulonephritis and retained renal function.[11] Thus, the possibility that precursor secretion from the intestine or other organs is increased in nephrotic syndrome could not be excluded.

To clarify whether the receptor is upregulated in nephrotic syndrome, we examined GC-C mRNA expression in the kidneys. However, the levels of GC-C mRNA in the kidney were too low on day 6 to compare uroguanylin-treated and untreated nephrotic rats (data not shown). In addition, urinary excretion and tissues levels of cGMP, an intracellular second messenger of uroguanylin, were not increased in uroguanylin-treated rats (group IV) compared with untreated (group III) nephrotic rats. Uroguanylin signalling in the kidney remains obscure, but our results suggested that uroguanylin acts via a GC-C independent pathway for urinary sodium excretion in nephrosis. Recent reports have indicated that some GC-C independent pathways exist because the effect of uroguanylin on the kidney persists in mice lacking GC-C.[7,19–24] Uroguanylin acts through a GC-C-independent, cGMP-dependent mechanism in mice lacking the GC-C receptor.[7] However, the levels of cGMP did not change in our study, so other cGMP-independent pathways might be associated with nephrosis. ANP, which is one of the most potent of the natriuretic factors, is produced mainly in the cardiac atria and elicits natriuresis by activating the transmembranous guanylate cyclase, GC-A, which results in increased intracellular cGMP. The effect of infused ANP is reduced in nephrotic syndrome because cGMP-phosphodiesterase (PDE) activity, which catabolizes and removes cGMP, is increased in nephrosis.[25] On the other hand, uroguanylin might work via the cGMP-independent pathway, and be able to induce natriuresis in the nephrotic kidney.

In conclusion, uroguanylin increased urinary sodium excretion in rats with PAN-induced nephrosis. Further studies are warranted to clarify the mechanisms of uroguanylin action in the nephrotic kidney. However, uroguanylin plays an important role as a natriuretic factor in nephrotic syndrome, and might be a useful novel agent for treating conditions associated with sodium retention.

ACKNOWLEDGEMENTS

This study was supported by Grants-in-Aid for Scientific Research from the Ministry of Education, Science, Sports and Culture in Japan.

REFERENCES

1. Forte LR, London RM, Freeman RH, Krause WJ. Guanylin peptides: Renal actions mediated by cyclic GMP. *Am. J. Physiol. Renal Physiol.* 2000; **278**: F180–91.
2. Forte LR. Uroguanylin and guanylin peptides: Pharmacology and experimental therapeutics. *Pharmacol. Ther.* 2004; **104**: 137–62.
3. Fan X, Wang Y, London RM *et al.* Signaling pathways for guanylin and uroguanylin in the digestive, renal, central nervous, reproductive, and lymphoid systems. *Endocrinology* 1997; **138**: 4636–48.
4. Fonteles MC, Greenberg RN, Monteiro HAS, Currie MG, Forte LR. Natriuretic and kaliuretic activities of guanylin and uroguanylin in the isolated perfused rat kidney. *Am. J. Physiol.* 1998; **275**: F191–7.
5. Greenberg RN, Hill M, Crytzer J *et al.* Comparison of effects of uroguanylin, guanylin, *Escherichia coli* heart-stable enterotoxin STa in mouse intestine and kidney: Evidence that uroguanylin is an intestinal natriuretic hormone. *J. Investig. Med.* 1997; **45**: 276–82.
6. Carrithers SL, Hill MJ, Johnson BR *et al.* Renal effects of uroguanylin and guanylin *in vivo*. *Braz. J. Med. Biol. Res.* 1999; **32**: 1337–44.
7. Carrithers SL, Ott CE, Hill MJ *et al.* Guanylin and uroguanylin induce natriuresis in mice lacking guanylyl cyclase-C receptor. *Kidney Int.* 2004; **65**: 40–53.
8. Fukae H, Kinoshita H, Fujimoto S, Kita T, Nakazato M, Eto T. Changes in urinary levels and renal expression of uroguanylin on low or high salt diets in rats. *Nephron* 2002; **92**: 373–8.
9. Kita T, Kitamura K, Sakata J, Eto T. Marked increased of guanylin secretion in response to salt loading in the rat small intestine. *Am. J. Physiol.* 1999; **277**: G960–6.
10. Lorenz JN, Nieman M, Sabo J *et al.* Uroguanylin knockout mice have increased blood pressure and impaired natriuretic response to enteral NaCl load. *J. Clin. Invest.* 2003; **112**: 1244–54.
11. Kinoshita H, Fujimoto S, Kita T *et al.* Urine and plasma levels of uroguanylin and its molecular forms in renal disease. *Kidney Int.* 1997; **52**: 1028–34.
12. Kinoshita H, Fujimoto S, Fukae H *et al.* Plasma and urine levels of uroguanylin, a new natriuretic peptide, in nephrotic syndrome. *Nephron* 1999; **81**: 160–64.
13. Carrithers SL, Eber SL, Forte LR, Greenberg RN. Increased urinary excretion of uroguanylin in patients with congestive heart failure. *Am. J. Physiol. Heart Circ. Physiol.* 2000; **278**: H538–47.
14. Nakazato M, Yamaguchi H, Kinoshita H *et al.* Identification of biologically active and inactive human uroguanylin in plasma and urine and their increases in renal insufficiency. *Biochem. Biophys. Res. Commun.* 1996; **220**: 586–93.
15. Kikuchi M, Fujimoto S, Fukae H *et al.* Rule of uroguanylin, a peptide with natriuretic activity, in rats with experimental nephritic syndrome. *J. Am. Soc. Nephrol.* 2005; **16**: 392–7.
16. Perico N, Remuzzi G. Edema of the nephrotic syndrome: The role of the atrial peptide system. *Am. J. Kidney Dis.* 1993; **22**: 355–66.
17. Perico N, Delaini F, Lupini C *et al.* Blunted excretory response to atrial natriuretic peptide in experimental nephrosis. *Kidney Int.* 1989; **36**: 57–64.
18. Keller E, Hoppe-Seyler G, Shollmeyer P. Disposition and diuretic effect of furosemide in nephrotic syndrome. *Clin. Pharmacol. Ther.* 1982; **32**: 442–9.
19. Sindic A, Basoglu C, Cerci A *et al.* Guanylin, uroguanylin, and heat-stable euterotoxin activate guanylate cyclase C and/or a pertussis toxin-sensitive G protein in human proximal tubule cells. *J. Biol. Chem.* 2002; **277**: 17758–64.
20. Sindic A, Velic A, Basoglu C *et al.* Uroguanylin and guanylin regulate transport of mouse cortical collecting duct independent of guanylate cyclase C. *Kidney Int.* 2005; **68**: 1008–17.
21. Sindic A, Hirsch JR, Velic A, Piechota H, Schlatter E. Guanylin and uroguanylin regulate electrocyte transport in isolated human cortical collecting ducts. *Kidney Int.* 2005; **67**: 1420–27.
22. Elitsur N, Lorenz JN, Hawkins JA *et al.* The proximal convoluted tubule is a target for the uroguanylin-regulated natriuretic response. *J. Pediatr. Gastroenterol. Nutr.* 2006; **43**: S74–81.
23. Sindic A, Schlatter E. Cellular effects of guanylin and uroguanylin. *J. Am. Soc. Nephrol.* 2006; **17**: 607–16.
24. Sindic A, Schlatter E. Mechanisms of action of uroguanylin and guanylin and their role in salt handling. *Nephrol. Dial. Transplant.* 2006; **21**: 3007–12.
25. Valentin JP, Ying WZ, Sechi L *et al.* Phosphodiesterase inhibitors correct resistance to natriuretic peptides in rats with Heymann nephritis. *J. Am. Soc. Nephrol.* 1996; **7**: 582–93.

Biochemical and Biophysical Research Communications 384 (2009) 249–254

Contents lists available at ScienceDirect

Biochemical and Biophysical Research Communications

journal homepage: www.elsevier.com/locate/ybbrc

Flow cytometric analysis of the calcitonin receptor-like receptor domains responsible for cell-surface translocation of receptor activity-modifying proteins

Kenji Kuwasako [a,*], Kazuo Kitamura [b], Sayaka Nagata [b], Johji Kato [a]

[a] Frontier Science Research Center, University of Miyazaki, 5200 Kihara, Kiyotake, Miyazaki 889-1692, Japan
[b] Circulation and Body Fluid Regulation, Faculty of Medicine, University of Miyazaki, 5200 Kihara, Kiyotake, Miyazaki 889-1692, Japan

ARTICLE INFO

Article history:
Received 20 April 2009
Available online 24 April 2009

Keywords:
Receptor activity-modifying proteins
Calcitonin receptor-like receptor
Chimeric receptor
Translocation
Flow cytometry

ABSTRACT

The three receptor activity-modifying proteins (RAMPs1, -2, and -3) associate with a wide variety of G protein-coupled receptors (GPCRs), including calcitonin receptor-like receptor (CRLR). In this study, we used flow cytometry to measure RAMP translocation to the cell surface as a marker of RAMP–receptor interaction. Because VPAC2 does not interact with RAMPs, although, like CRLR, it is a Family B peptide hormone receptor, we constructed a set of chimeric CRLR/VPAC2 receptors to evaluate the trafficking interactions between CRLR domains and each RAMP. We found that CRLR regions extending from transmembrane domain 1 (TM1) through TM5 are necessary and sufficient for the transport of RAMPs to the plasma membrane. In addition, the extracellular N-terminal domain of CRLR, its 3rd intracellular loop and/or TM6 were also important for the cell-surface translocation of RAMP2, but not RAMP1 or RAMP3. Other regions within CRLR were not involved in trafficking interactions with RAMPs. These findings provide new insight into the trafficking interactions between accessory proteins such as RAMPs and their receptor partners.

Introduction

Receptor activity-modifying proteins (RAMPs1, -2 and -3) were the first accessory proteins known to modulate the function of G protein-coupled receptors (GPCRs) [1]. In mammals, all three RAMPs are comprised of ~160 amino acids and exhibit a common structure consisting of a large extracellular N-terminal domain, a single membrane-spanning domain and a short cytoplasmic C-terminal tail. However, the three isoforms share less than 30% sequence identity [1,2], differ with respect to their expression levels in tissues, and are differentially affected by various pathological conditions [2].

RAMPs were first identified as chaperones promoting the forward trafficking of calcitonin receptor-like receptor (CRLR; a Family B GPCR) and calcium sensing receptor (a Family C GPCR) from the endoplasmic reticulum to the cell surface [1–3]. Once at the cell surface, RAMPs govern the expression of the GPCR phenotype [2,4]. For example, CRLR/RAMP1 and CRLR/RAMP2 or -3 function as calcitonin gene-related peptide (CGRP) and adrenomedullin (AM) receptors, respectively [1,2]. Both agonists are potent vasodilators that also have been shown to exert powerful protective effects against multi-organ damage [2,5].

RAMPs can also interact strongly with Family B GPCRs able to translocate to the cell surface without a chaperone [2,4]. For example, expression of the calcitonin (CT) receptor with RAMP1, -2 or -3 produces three subtypes of high-affinity amylin receptor [2,4]. All three RAMPs strongly interact with the vasoactive intestinal peptide (VIP)/pituitary adenylate cyclase-activating polypeptide type 1 receptor (VPAC1) with no effect on the receptor's pharmacology [2,4]. The parathyroid hormone 1 (PTH1) and glucagon receptors are known to selectively interact with RAMP2, while the PTH2 receptor selectively interacts with RAMP3 [2,4].

We previously demonstrated the utility of flow cytometry for evaluating the trafficking interactions between CRLR and various RAMP mutants [6,7]. However, little is known about the trafficking interactions between specific CRLR domains and each of three RAMPs. In the present study, therefore, we generated chimeric receptors by exchanging regions of CRLR with the corresponding sequences of VPAC2, which our flow cytometric analysis showed does not interact with any V5-tagged RAMPs in human embryonic kidney (HEK)-293 cells. Our analysis revealed not only the key CRLR domains responsible for cell-surface translocation of each RAMP, but also differences in the RAMP–CRLR interactions among the three RAMPs.

* Corresponding author. Fax: +81 985 85 9718.
E-mail address: kuwasako@fc.miyazaki-u.ac.jp (K. Kuwasako).

0006-291X/$ - see front matter © 2009 Elsevier Inc. All rights reserved.
doi:10.1016/j.bbrc.2009.04.097

Materials and methods

Regents and antibodies. Human (h)VIP and αCGRP were purchased from the Peptide Institute (Osaka, Japan). Human AM was kindly donated by Shionogi & Co. (Osaka, Japan). Mouse anti-V5 antibody and FITC-conjugated mouse anti-V5 monoclonal antibody (anti-V5-FITC antibody) were purchased from Invitrogen.

Expression constructs and chimers. Human VPAC2 (GenBank Accession No. L40764) was cloned from cDNA obtained from human small intestine (Clonthech) by PCR using appropriate primers and then modified to provide a consensus Kozak sequence as previously described [8]. The expression vector pCAGGS-VPAC2 was then constructed by cloning VPAC2 cDNA into the mammalian vector pCAGGS/Neo using the 5′ XhoI and 3′ NotI sites [8]. In addition, a double V5 epitope tag was ligated, in-frame, to the 5′ end of the VPAC2 cDNA, and the native signal sequences were replaced with the influenza hemagglutinin signal sequence [8], after which the V5-VPAC2 was cloned into pCAGGS/Neo. In similar fashion, wild-type and double V5-tagged constructs for hCRLR and each RAMP were cloned into pCAGGS/Neo [6,9]. Because V5-RAMP3 was more strongly expressed at the cell surface than V5-RAMP1 or -2, even when transfected alone into HEK-293 cells [6], a double V5 epitope tag was inserted between amino acids 33 and 34 in the hRAMP3 N-terminus, as described previously [10].

Nine CRLR/VPAC2 chimeras (CH1–CH9) were constructed utilizing seven restriction sites. Human CRLR naturally possesses three sites (at two positions distal to the N-terminus and TM2, respectively and at a position proximal to the C-terminus); the remaining four sites (at positions distal to TM3, -4, -5 and -6, respectively) were introduced without altering the amino acid sequence of the receptor. VPAC2 shares only 30% amino acid sequence identity with hCRLR and contains none of these sites. Therefore, corresponding VPAC2 fragments containing these restriction sites were prepared by PCR using primers containing the sites. The separate fragments of CRLR and VPAC2 were then ligated into the same expression vector.

The aforementioned gene constructs were all sequenced using an Applied Biosystems 310 Genetic Analyzer.

Cell culture and DNA transfection. HEK-293 or COS-7 cells were maintained in DMEM supplemented with 10% FBS, 100 U/ml penicillin G, 100 μg/ml streptomycin, 0.25 μg/ml amphotericin B at 37 °C under a humidified atmosphere of 95% air/5% CO_2. For experimentation, cells were seeded into 12- or 24-well plates and, upon reaching 70–80% confluence, were transiently transfected with the indicated cDNAs using LipofectAMINE transfection reagents (Invitrogen) according to the manufacturer's instructions. Expression vector constructs for the appropriate wild-type or chimeric receptor and each RAMP were cotransfected in equal amounts. As a control, some cells were transfected with empty vector (pCAGGS/Neo) (*Mock*). All of the experiments were performed 48 h after transfection.

Fluorescence-activated cell-sorting (FACS) analysis. To evaluate cell surface expression of the indicated V5-tagged constructs, cells grown in 12-well plates were harvested following transient transfection, washed twice with PBS, resuspended in ice-cold FACS buffer [8], and then incubated for 60 min at 4 °C in the dark with anti-V5-FITC antibody (1:1000 dilution). For evaluation of intracellular and/or surface expression of the aforementioned V5-tagged constructs, HEK-293 cells were first permeabilized using IntraPrep™ reagents (Beckman Coulter) according to the manufacturer's instructions and then incubated with anti-V5-FITC antibody (1:1000 dilution) for 15 min at room temperature in the dark. Following two successive washes, both groups of cells were subjected to flow cytometry in an EPICS XL flow cytometer (Beckman Coulter) [8].

Measurement of intracellular cAMP. In Hanks' buffer containing 20 mM Hepes and 0.2% bovine serum albumin, transfected cells were exposed to the indicated concentrations of hAM for 15 min at 37 °C in the presence of 0.5 mM 3-isobutyl-1-methylxanthine (Sigma). The reactions were terminated by addition of lysis buffer (GE Healthcare), after which the cAMP content was determined using a commercial enzyme immunoassay kit according to the manufacturer's instructions (GE Healthcare) for the non-acetylation protocol.

Statistical analysis. Results are expressed as means ± SEM of at least three independent experiments. Differences between two groups were evaluated using Student's *t*-tests; differences among multiple groups were evaluated using one-way analysis of variance followed by Scheffe's tests. Values of $p < 0.05$ were considered significant.

Results

Characterization of VPAC2 overexpressed in HEK-293 cells with or without RAMPs

When transfected into HEK-293 cells, VPAC2 mediated marked, concentration-dependent increases in cAMP in response to VIP (EC_{50} = 0.64 ± 0.03 nM) (Fig. 1A). But neither AM nor CGRP elicited cAMP production in VPAC2 transfectants (Fig. 1A), which was comparable to that seen in cells transfected with CRLR [6,11] or RAMP2 [11]. These findings confirm that our HEK-293 cells lack both functional RAMPs and CRLR, that the VPAC2 is unable to function as an AM or CGRP receptor. In the present study, therefore, we used FACS analysis of HEK-293 cells to evaluate the interaction between RAMP and VPAC2 or CRLR/VPAC2 chimeras.

We initially tested whether VPAC2 interacts with any of the three RAMPs. Surface binding of anti-V5-FITC antibody was within the 2% limit of resolution when cells were transfected with empty vector (*Mock*). When expressed alone FITC-labeled V5-CRLR was detected in ~30% of cells (Fig. 3). When co-expressed with wild-type RAMP1, -2 or -3, the surface expression frequency was significantly increased (Fig. 3). By contrast, the surface expression of V5-VPAC2 (42.2%) was not increased by co-transfection with RAMP1, -2 or -3 (39.2%, 39.8% and 38.8%, respectively) (not shown).

Subsequent comparison of the changes in the frequency of surface expression of V5-RAMP1, -2 and -3 co-transfected with wild-type CRLR or VPAC2 (Figs. 1A–C) revealed that surface expression of V5-RAMP1 and -2 was markedly increased by co-transfection of CRLR but not VPAC2. In contrast to V5-RAMP1 and -2, V5-RAMP3 appeared at the surface of 19.0% of cells when the protein was expressed alone, provably due to its self-transport to the cell surface [12] or its interaction with other endogenous GPCRs [2,4]. Still, although the cell surface expression of V5-RAMP3 was further increased by co-transfection of CRLR, it was unaffected by VPAC2. Thus the observed pattern of cell-surface expression is consistent with there being no interaction between VPAC2 and any of the three RAMPs.

FACS analysis of the trafficking interaction between RAMP and CRLR/VPAC2 chimeras

Because there are no interactions between VPAC2 and RAMPs, we constructed a set of nine chimeric CRLR/VPAC2 receptors (Fig. 2A) to evaluate the trafficking interactions between specific CRLR domains and each of RAMPs. These chimeras were then transiently co-transfected with each RAMP into HEK-293 cells, and their interaction was characterized using flow cytometry.

We initially analyzed the total expression of each of the V5-tagged chimera in permeabilized cells when transfected alone

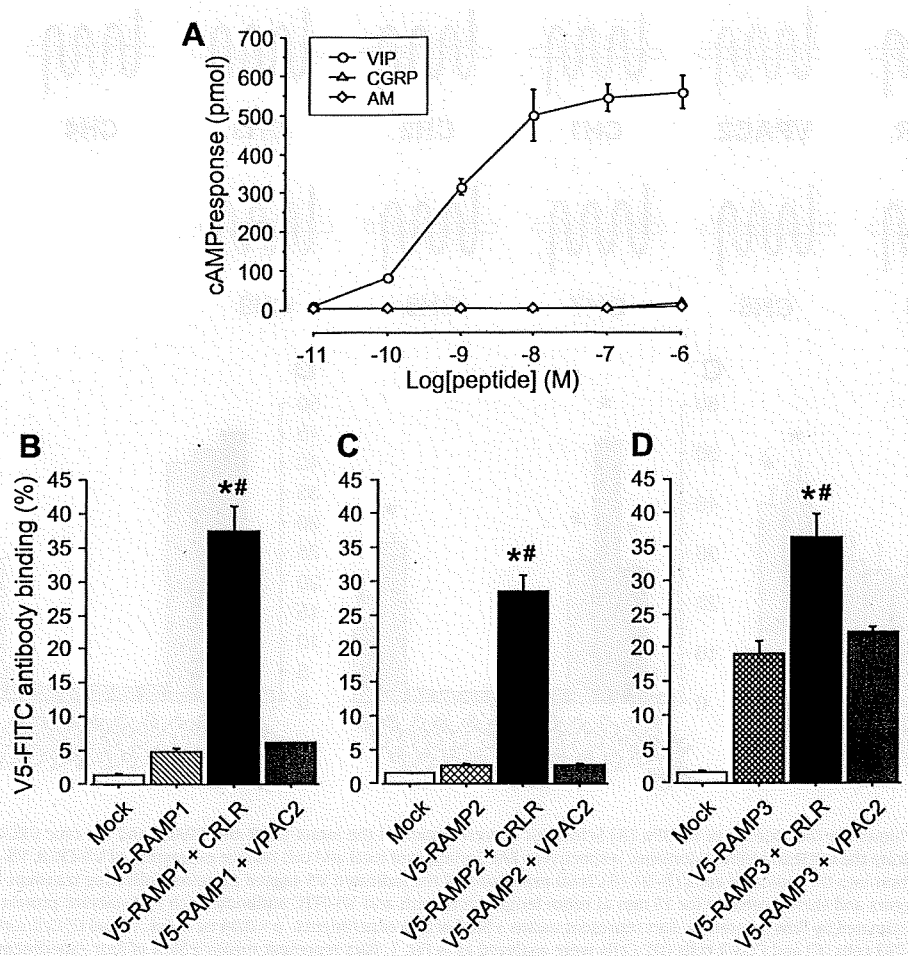

Fig. 1. Characterization of VPAC2 overexpressed in HEK-293 cells. (A) Agonist-evoked cAMP production in HEK-293 cells expressing VPAC2 alone. Cells were transiently transfected with VPAC2, after which they were stimulated with the indicated concentrations of VIP, CGRP or AM for 15 min at 37 °C and then lysed. The resultant lysates were analyzed for cAMP content. Bars represent means ± SEM of three experiments. FACS analysis of the cell surface expression of V5-RAMP1 (B), V5-RAMP2 (C) and V5-RAMP3 (D) following transfection into HEK-293 cells, with or without CRLR or VPAC2. Forty-eight hours after transfection, cells were incubated for 1 h at 4 °C with monoclonal anti-V5-FITC antibody; mock incubation with the antibody served as the control. FITC-labeled V5-CRLR and V5-VPAC2 expressed at the cell surface were separately estimated by flow cytometry. Bars represent means ± SEM of three to four experiments. $^{*}p < 0.0005$ vs. Mock; $^{\#}p < 0.001$ vs. the corresponding V5-RAMP alone.

(Fig. 2B). FITC-labeled CRLR was detected in 53.1% of cells, and similar results were observed in VPAC2 transfectants. Among the nine chimeras tested, full expression of CH1, -8 and -9 was detected in 38–45% of cells. Transfection of the remaining six chimeras led to their full expression in 25–31% of cells. Thus the transfection efficacies of the chimeras did not significantly differ from that of CRLR.

We next analyzed the cell surface expression of the V5-tagged constructs in non-permeabilized HEK-293 cells when expressed alone (Fig. 2C). FITC-labeled CRLR was detected in 27.4% of cells, despite of the absence of RAMPs, which is consistent with earlier observations [11,13]. V5-VPAC2 transfection led to its strong surface expression in 52.5% of cells. Surface expression of three chimeras, CH1, -8 and -9, was detected in 14–32% of cells. The remaining six chimeras appeared at the surface of only 2.0–2.6% of cells.

Although COS-7 cells express no functional RAMPs [3,14], there have been several reports showing that tagged CRLR is highly expressed at the cell surface when transfected alone [13,15]. As shown in Fig. 2D, V5-CRLR appeared at the surface of 45.2% of COS-7 cells, which was a higher frequency than in HEK-293 cells (Fig. 2C). Similar differences in surface receptor expression between these two cell types were also observed when the cells were transfected with chimeras CH1 and CH9. The cell surface expression of the other chimeras was similar to that seen in HEK-293 cells.

We also examined the effects of co-transfecting each wild-type RAMP on the surface expression of V5-tagged chimeras in HEK-293 cells (Fig. 3). Surprisingly, co-transfection of RAMP1, -2 or -3 led to markedly greater increases in surface delivery of two chimeras, CH6 and CH7, than was seen with V5-CRLR. On the other hand, co-transfection of RAMPs had no substantial effect on the cell-surface expression of the other chimers.

We next measured V5-RAMP translocation to the cell surface as a marker of RAMP–receptor interaction (Fig. 4). The surface expression of V5-RAMP1, -2 and -3 was markedly increased by co-transfection of two chimeras, CH7 and CH8. By contrast, co-transfection of CH2, -3, -4, -5 or -9 did not increase translocation of the three RAMPs. Co-transfection of CH1 significantly increased surface expression frequency of V5-RAMP1 to 29.4%, which is ~75% of that seen with CRLR. Similarly, CH1 increased the frequency of V5-RAMP3 surface expression to a level equal to that seen with CRLR, whereas CH1 did not significantly increase cell-surface delivery of V5-RAMP2. Co-transfection of CH6 markedly increased the frequency of surface expression of V5-RAMP1 and -3 to a level comparable to that seen with CRLR, while increases in surface expression of V5-RAMP2 mediated by CH6 were about half of those seen with CRLR.

Discussion

That surface expression of V5-CRLR in HEK-293 cells was significantly increased by co-transfection of each of the three RAMPs is

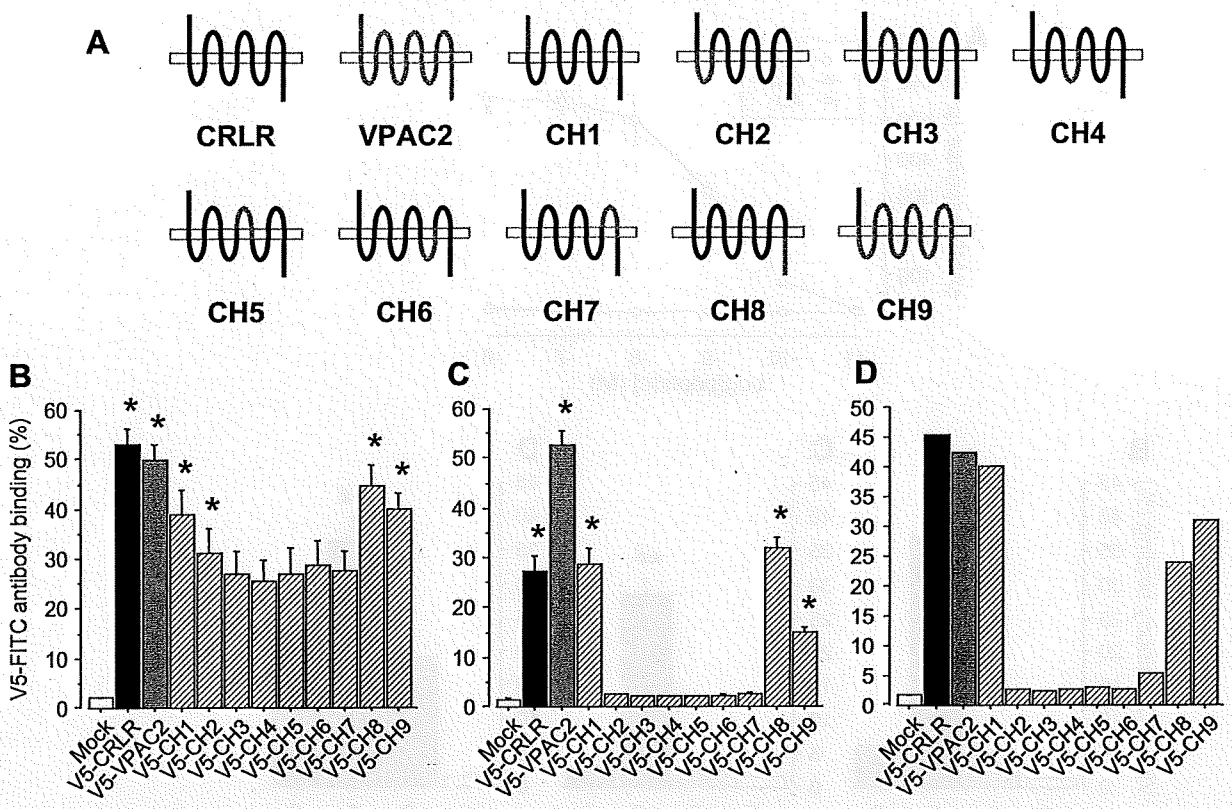

Fig. 2. Characterization of CRLR/VPAC2 chimers in the absence of RAMPs. (A) Schematic representation of the intact CRLR and VPAC2 and the nine CRLR/VPAC2 chimeras (CH1–CH9). Bold black and gray lines indicate the CRLR and VPAC2 domains, respectively. FACS analysis of total and cell surface expression of V5-CRLR, V5-VPAC2 or the V5-CRLR/VPAC2 chimeras following transfection into the indicated cells (B–D). (B) Total expression of the indicated V5-tagged proteins. Following transient transfection, cells were permeabilized with IntraPrep™ reagents and then incubated for 15 min at room temperature with anti-V5-FITC antibody. Each FITC-labeled protein expressed in the cytoplasm and/or at the cell surface was estimated by flow cytometry. Bars represent means ± SEM of four experiments. $^{*}p < 0.04$ vs. Mock. (C and D) Cell surface expression of the indicated V5-tagged proteins in HEK-293 cells (C) and COS-7 cells (D). Cells were analyzed as in Fig. 1. Bars represent means ± SEM of four experiments for (C) and two experiments for (D). $^{*}p < 0.01$ vs. Mock.

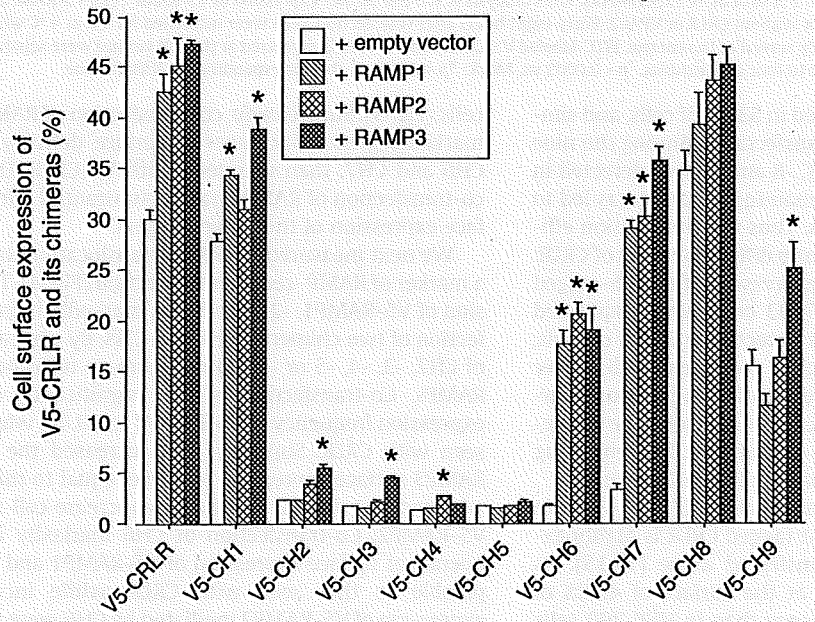

Fig. 3. FACS analysis of cell surface expression of V5-CRLR and the V5-CRLR/VPAC2 chimeras following transfection into HEK-293 cells, with or without RAMP1, -2 or -3. After transfection, cells were analyzed as in Fig. 1. Bars represent means ± SEM of three experiments. $^{*}p < 0.05$ vs. the corresponding V5-CRLR alone or V5-CRLR/VPAC2 chimera alone.

indicative of the trafficking interactions between CRLR and RAMPs (Fig. 3). Each of the RAMPs can also associate with the CT receptor, thereby forming three functional amylin receptors [2,14]. But surface expression of the CT receptor is not increased by co-transfec-

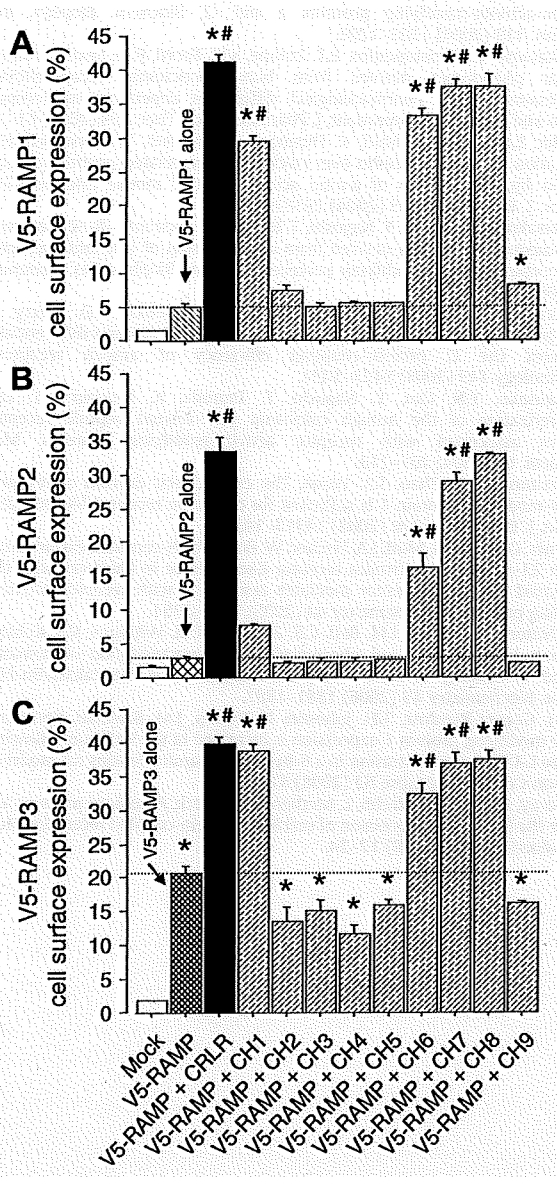

Fig. 4. FACS analysis of the cell surface expression of V5-RAMP1 (A), V5-RAMP2 (B), and V5-RAMP3 (C) following transfection into HEK-293 cells, with or without CRLR or CRLR/VPAC2 chimeras. After transfection, cells were analyzed as in Fig. 1. Bars represent means ± SEM of three experiments. $^{*}p < 0.03$ vs. Mock; $^{\#}p < 0.005$ vs. the corresponding V5-RAMP alone.

tion with RAMP in HEK-293 cells [16] or COS-7 cells [17], reflecting the efficient self-transport of the CT receptor to the cell surface. Our present findings show that the self-transport of VPAC2 is very similar to that of the CT receptor. Notably, overexpression of the CT receptor leads to marked increases in the surface delivery of V5-RAMPs [12,18], but overexpression of VPAC2 did not. Thus translocation of GPCRs to the cell surface may not be a useful marker of RAMP–GPCR interaction. On the other hand, surface delivery of V5-RAMP1, -2 and -3 in HEK-293 cells was markedly increased by co-transfection of CRLR. These increases were more dramatic than those seen when V5-CRLR was co-transfected with each of the three RAMPs. Thus using FACS to measure the surface delivery of tagged RAMPs co-expressed with GPCRs appears to be an effective means of evaluating trafficking interactions between RAMPs and GPCRs.

In the present study, co-transfection of four chimeras, CH2, -3, -4 and -5, did not lead to increases in cell-surface expression of V5-RAMP1, -2 or -3. Nonetheless, total expression of these chimeras did not significantly differ from that of CRLR in the absence of exogenous RAMPs (Fig. 2B), which suggests that the absence of the surface delivery of V5-RAMPs was not due to diminished synthesis of these chimeras or to their enhanced degradation (e.g., due to misfolding). Collectively then, these results indicate that regions extending from TM1 through TM5 within CRLR are necessary and sufficient for the transport of RAMPs to the plasma membrane. Additional FACS analysis will be needed to determine in detail the specific regions of CRLR involved in their trafficking interactions with RAMPs.

The CRLR/VPAC2 chimera CH9, in which the N-terminus of VPAC2 was replaced with that of CRLR, also failed to increase cell-surface translocation of the three V5-RAMPs in HEK-293 cells. This is consistent with the results obtained with CH2, -3, -4 and -5, probably reflects the presence of VPAC2 sequences in regions extending from TM1 through TM5 in the CH9. Like VPAC2, the secretin and PTH receptors, both of which are Family B GPCRs, do not associate with RAMP1 [4,19]. In contrast to our results, an earlier immunoblot analysis showed that two chimeras in which the N-termini of the secretin and PTH receptors were replaced with that of CRLR, appeared at the cell surface along with RAMP1 in both HEK-293 (tsA 201) [19] and COS-7 [20] cells. On the other hand, neither chimera was capable of signaling with CGRP, despite the fact that both CGRP and a non-peptide CGRP antagonist interact directly with the N-terminus of CRLR in complex with RAMP1 [20,21]. The inconsistency of the data likely reflects differences in chimeric GPCR partners, cell types, and assays of RAMP translocation to the cell surface.

We fond that chimeras CH1, -6, -7 and -8, which possess no VPAC2 sequences in regions extending from TM1 to TM5, increased the surface expression of V5-RAMP1 and -3 to the same degree as CRLR did. Interestingly, CH7 and CH8, but not CH1 or CH6, also increased surface delivery of V5-RAMP2, indicating that the N-terminus, 3rd intracellular loop and/or TM6 within CRLR are also important for selective trafficking interactions with RAMP2. Human RAMP2 is 26 amino acids longer than either hRAMP1 or hRAMP3, and hRAMP1 and -3, but not hRAMP2, possess 11 conserved amino acids in their N-terminus and TM domains [1,2]. The unique features of RAMP2 likely account for its specific trafficking interactions with CRLR.

In summary, we have shown that using flow cytometry to measure cell-surface translocation of the three RAMPs is an effective means of evaluating RAMP–receptor interactions, irrespective of whether GPCRs are capable of self-transport (e.g., CRLR vs. CT receptor). The present FACS analysis also revealed the crucial CRLR regions (from TM1 to TM5) responsible for cell-surface translocation of RAMPs, as well as the differences in trafficking interactions among RAMPs with respect to the N-terminus, 3rd intracellular loop and/or TM6 of CRLR.

Notably, recent work suggests there may be a relationship between RAMP1 and the dopamine receptor, a Family A GPCR [22]. To date, at least seven types of accessory protein, including RAMPs, have been shown to be required for correct targeting of GPCRs to the cell surface [23]. The present FACS analysis should therefore contribute greatly to the identification of additional RAMP-interacting GPCRs, and may also stimulate investigation of other interactions between accessory proteins and their receptor partners.

Acknowledgments

This work was supported in part by a Grant-in-Aid for Scientific Research from the Ministry of Education, Culture, Sports and Science.

References

[1] L.M. McLatchie, N.J. Fraser, M.J. Main, A. Wise, J. Brown, N. Thompson, R. Solari, M.G. Lee, S.M. Foord, RAMPs regulate the transport and ligand specificity of the calcitonin-receptor-like receptor, Nature 393 (1998) 333–339.

[2] D.L. Hay, D.R. Poyner, P.M. Sexton, GPCR modulation by RAMPs, Pharmacol. Ther. 109 (2006) 173–197.
[3] T. Bouschet, S. Martin, J.M. Henley, Regulation of calcium-sensing-receptor trafficking and cell-surface expression by GPCRs and RAMPs, Trends Pharmacol. Sci. 29 (2008) 633–639.
[4] P.M. Sexton, D.R. Sexton, J. Simms, A. Christopoulos, D.L. Hay, Modulating receptor function through RAMPs: can they represent drug targets in themselves?, Drug Discov Today 14 (2009) 413–419.
[5] C. Gibbons, R. Dackor, W. Dunworth, K. Fritz-Six, K.M. Caron, Receptor activity-modifying proteins: RAMPing up adrenomedullin signaling, Mol. Endocrinol. 21 (2007) 783–796.
[6] K. Kuwasako, K. Kitamura, S. Nagata, J. Kato, Functions of the extracellular histidine residues of receptor activity-modifying proteins vary within adrenomedullin receptors, Biochem. Biophys. Res. Commun. 377 (2008) 109–113.
[7] K. Kuwasako, K. Kitamura, Y. Nagoshi, Y.N. Cao, T. Eto, Identification of the human receptor activity-modifying protein 1 domains responsible for agonist binding specificity, J. Biol. Chem. 278 (2003) 22623–22630.
[8] K. Kuwasako, Y. Shimekake, M. Masuda, K. Nakahara, T. Yoshida, M. Kitaura, K. Kitamura, T. Eto, T. Sakata, Visualization of the calcitonin receptor-like receptor and its receptor activity-modifying proteins during internalization and recycling, J. Biol. Chem. 275 (2000) 29602–29609.
[9] K. Kuwasako, Y.N. Cao, C.P. Chu, S. Iwatsubo, T. Eto, K. Kitamura, Functions of the cytoplasmic tails of the human receptor activity-modifying protein components of calcitonin gene-related peptide and adrenomedullin receptors, J. Biol. Chem. 281 (2006) 7205–7213.
[10] A. Christopoulos, G. Christopoulos, M. Morfis, M. Udawela, M. Laburthe, A. Couvineau, K. Kuwasako, N. Tilakarayne, P.M. Sexton, Novel receptor partners and function of receptor activity-modifying proteins, J. Biol. Chem. 278 (2003) 3293–3297.
[11] K. Kuwasako, K. Kitamura, T. Uemura, Y. Nagoshi, J. Kato, T. Eto, The function of extracellular cysteines in the human adrenomedullin receptor, Hypertens. Res. 26 (2003) S25–S31.
[12] M. Flahaut, B.C. Rossier, D. Firsov, Respective roles of calcitonin receptor-like receptor (CRLR) and receptor activity-modifying proteins (RAMP) in cell surface expression of CRLR/RAMP heterodimeric receptors, J. Biol. Chem. 277 (2002) 14731–14737.
[13] L.M. Itter, F. Luessi, D. Koller, W. Born, J.A. Fischer, R. Muff, Asparate^{69} of the calcitonin-like receptor is required for its functional expression together with receptor-activity-modifying proteins 1 and -2, Biochem. Biophys. Res. Commun. 319 (2004) 1203–1209.
[14] N. Tilakaratne, G. Christopoulos, E.T. Zumpe, S.M. Foord, P.M. Sexton, Amilyn receptor phenotypes derived from human calcitonin receptor/RAMP coexpression exhibit pharmacological differences dependent on receptor isoform and host cell environment, J. Pharmacol. Exp. Ther. 294 (2000) 61–72.
[15] D. Koller, L.M. Ittner, R. Muff, K. Husmann, J.A. Fischer, W. Born, Selective inactivation of adrenomedullin over calcitonin gene-related peptide receptor function by the deletion of amino acids 14–20 of mouse calcitonin-like receptor, J. Biol. Chem. 279 (2004) 20387–20391.
[16] K. Kuwasako, K. Kitamura, Y. Nagoshi, T. Eto, Novel calcitonin-(8-32)-sensitive adrenomedullin receptors derived from co-expression of calcitonin receptor with receptor activity-modifying proteins, Biochem. Biophys. Res. Commun. 301 (2003) 460–464.
[17] M. Morfis, N. Tilakaratne, S.G. Furness, G. Christopoulos, T.D. Werry, A. Christopoulos, P.M. Sexton, Receptor activity-modifying proteins differentially modulates the G protein-coupling efficiency of amylin receptors, Endocrinology 149 (2008) 5423–5431.
[18] K. Kuwasako, Y.N. Cao, Y. Nagoshi, T. Tsuruda, K. Kitamura, T. Eto, Characterization of the human calcitonin gene-related peptide receptor subtypes associated with receptor activity-modifying proteins, Mol. Pharmacol. 65 (2004) 207–213.
[19] T.J. Fitzsimmons, X. Zhao, S.A. Wank, The extracellular domain of receptor activity-modifying protein 1 is sufficient for calcitonin receptor-like receptor function, J. Biol. Chem. 278 (2003) 14313–14320.
[20] L.M. Ittner, D. Koller, R. Muff, J.A. Fischer, W. Born, The N-terminal extracellular domain 23–60 of the calcitonin receptor-like receptor in chimeras with the parathyroid hormone receptor mediates association with receptor activity-modifying protein 1, Biochemistry 44 (2005) 5749–5754.
[21] C.A. Salvatore, J.J. Mallee, I.M. Bell, C.B. Zartman, T.M. Williams, K.S. Koblan, S.A. Kane, Identification and pharmacological characterization of domains involved in binding of CGRP receptor antagonists to the calcitonin-like receptor, Biochemistry 45 (2006) 1881–1887.
[22] J. Lee, J. Gomez-Ramirez, T.H. Johnson, N. Visanji, J.M. Brotchie, Receptor-activity modifying protein 1 expression is increased in the striatum following repeated L-DOPA administration in a 6-hydroxydopamine lesions rat model of Parkinson's disease, Synapse 62 (2008) 310–313.
[23] S.N. Cooray, L. Chan, T.R. Webb, L. Metherell, A.J. Clark, Accessory proteins are vital for the functional expression of certain G protein-coupled receptors, Mol. Cell. Endocrinol. 300 (2009) 17–24.

Hypertension Research (2009) 32, 597–603

www.nature.com/hr

ORIGINAL ARTICLE

Pressure-independent effects of pharmacological stimulation of soluble guanylate cyclase on fibrosis in pressure-overloaded rat heart

Hiroyuki Masuyama[1], Toshihiro Tsuruda[1], Yoko Sekita[1], Kinta Hatakeyama[2], Takuroh Imamura[1], Johji Kato[3], Yujiro Asada[2], Johannes-Peter Stasch[4] and Kazuo Kitamura[1]

Cardiac fibrosis is a hallmark of cardiovascular remodeling associated with hypertension. The purpose of this study was to explore the effect and mechanism of soluble guanylate cyclase (sGC) stimulator BAY 41–2272, leading to intracellular cyclic guanosine monophosphate (cGMP) elevation, on the remodeling process induced by pressure overload. Seven-week-old male Wistar rats with hypertension induced by suprarenal aortic constriction (AC) were treated orally with 2 mg kg^{-1} day^{-1} of BAY 41–2272 for 14 days. BAY 41–2272 had no effects on blood pressure, but decreased AC-induced collagen accumulation in the left ventricle (LV), inhibiting the number of myofibroblasts and gene expressions of transforming growth factor-β1 and type 1 collagen. In addition, the antifibrotic action of BAY 41–2272 was accompanied by reducing AC-induced angiotensin-converting enzyme (ACE) mRNA and its enzymatic activity, and angiotensin II concentration in LV. In cultured cardiac fibroblasts, BAY 41–2272 inhibited ACE synthesis and myofibroblast transformation, accompanied by elevating the intracellular cGMP concentration. These results suggest that sGC stimulator BAY 41–2272 might be effective to reduce fibrosis in hypertensive heart disease by attenuating angiotensin II generation through myofibroblast transformation.
Hypertension Research (2009) **32**, 597–603; doi:10.1038/hr.2009.64; published online 8 May 2009

Keywords: angiotensin; cGMP; fibrosis; soluble guanylate cyclase

INTRODUCTION

Extracellular matrix mainly produced by fibroblasts is essential for organizing an elastic network of cardiocytes in the myocardium, while the structural and functional alteration of these cell types is important in the pathogenesis of hypertensive heart disease, characterized by the left ventricular (LV) hypertrophy and fibrosis.[1–3] As excessive myocardial fibrosis is assumed to be a critical determinant of the deterioration of LV function[4,5] and the cause of arrhythmias,[6] regulating the proliferation and activation of fibroblasts would be an important therapeutic target in the disorder. The renin–angiotensin II (Ang II) system (RAS) is recognized to stimulate fibrosis,[7] whereas the inhibition of either angiotensin-converting enzyme (ACE) or Ang II type 1 receptor has been shown to regress myocardial fibrosis in patients with hypertensive heart disease.[5,8]

Guanylate cyclase is an enzyme that converts guanosine triphosphate to cyclic guanosine monophosphate (cGMP). Both types of guanylate cyclase, particulate guanylate cyclase stimulated by atrial and brain natriuretic peptides,[9–13] and soluble guanylate cyclase (sGC) activated by nitric oxide,[9,14] are reported to attenuate cardiovascular remodeling by elevating intracellular cGMP levels. In an effort to develop agents activating sGC, BAY 41–2272 was identified as an orally active nitric oxide-independent stimulator of the sGC α1-subunit.[15] We and others have shown the beneficial effects of this compound not only on hemodynamics, but also on cardiovascular remodeling.[15–18] As sGC/cGMP activation has been shown to interfere with RAS,[19,20] we tested the hypothesis that the direct stimulation of sGC with BAY 41–2272 could attenuate myocardial fibrosis by inhibiting RAS activation. In this study, we used rats with pressure overload induced by suprarenal aortic constriction (AC), a model of hypertensive heart disease accompanied by fibroblast and RAS activation.[21]

METHODS

This study was performed in accordance with the Animal Welfare Act and approval from the University of Miyazaki Institutional Animal Care and Use Committee (2006-014). This investigation also conformed to the Guide for the Care and Use of Laboratory Animals published by the US National Institutes of Health (NIH Publication No. 85-23, revised 1996).

[1]Department of Internal Medicine, Circulatory and Body Fluid Regulation, Faculty of Medicine, University of Miyazaki, Miyazaki, Japan; [2]Department of Pathology, Faculty of Medicine, University of Miyazaki, Miyazaki, Japan; [3]Frontier Science Research Center, University of Miyazaki, Miyazaki, Japan and [4]PharmD at Cardiovascular Research, Bayer HealthCare, Aprather Weg 18a, Wuppertal, Germany
Correspondence: Dr T Tsuruda, Department of Internal Medicine, Circulatory and Body Fluid Regulation, Faculty of Medicine, University of Miyazaki, 5200 Kihara Kiyotake, Miyazaki 889-1692, Japan.
E-mail: ttsuruda@med.miyazaki-u.ac.jp
Received 22 October 2008; revised 27 February 2009; accepted 7 April 2009; published online 8 May 2009

Animal experiment

Seven-week-old male Wistar rats (Charles River, Yokohama, Japan), weighing 200–250 g, were housed in a temperature and light-controlled room (25 ± 1 °C; 12/12-h light/dark cycle) for 1 week before use, with free access to normal rat chow and water. The rats were divided into three groups: control group (n=11) and two pressure-overloaded groups with (n=21) or without (n=15) BAY 41–2272 treatment. Pressure overload was induced by abdominal AC at the suprarenal level, as described earlier.[22] In brief, a 22-gauge needle was placed adjacent to the abdominal aorta proximal to the renal artery, and ligated tightly around the aorta and the adjacent needle. The needle was then removed, leaving the vessel constricted to the diameter of the needle. The control group underwent identical surgical procedures but without constriction of the aorta. BAY 41–2272 compound, supplied by Bayer HealthCare (Wuppertal, Germany), was given by gastric gavage at a sub-depressor dose of 2 mg kg^{-1} twice a day for 14 days. The dose of BAY 41–2272 was chosen according to our earlier study.[18] The Datascience telemetric system (St Paul, MN, USA) was used to monitor the blood pressure of four unrestricted, conscious rats in each study group, as described earlier.[23] After banding the abdominal aorta, the transmitter catheter (model TA11PA-C40) was inserted into the descending aorta through the left carotid artery, and then the transmitter was implanted in the peritoneal cavity. After surgery, each rat was kept in an individual cage placed on a telemetric receiver pad. Blood pressure and heart rate data were collected for 10 s every 15 min and daily averages were calculated. At day 14, rats were anesthetized with pentobarbital sodium and killed by drawing blood from the thoracic aorta. After the whole heart was weighed, LV was frozen in liquid nitrogen or fixed in 4% paraformaldehyde and embedded in paraffin wax.

Immunohistochemistry and histological analysis

Immunohistochemical staining for α-smooth muscle actin (α-SMA) and ACE were performed as described earlier.[18,24] Slides were stained with mouse anti-α-SMA monoclonal antibody (1:200, Clone 1A4, DakoCytomation, Carpinteria, CA, USA) or rabbit polyclonal antibody against ACE (1:100, Santa Cruz Biotechnology, Santa Cruz, CA, USA) overnight at 4 °C. After the overnight reaction with antibodies, slide sections were incubated with EnVision+ (Dako) for 30 min, visualized with 0.05% 3,3-diaminobenzidine containing hydrogen peroxide, and counterstained with hematoxylin. Myofibroblasts positive for α-SMA were counted at ×200 magnification. To detect collagen fibers, slides were incubated with 0.1% picrosirius red (Direct Red 80, Sigma, St Louis, MO, USA) dissolved in saturated picric acid for 10 min, as described earlier.[18] To measure cardiocyte size, cross-sectional areas of ⩾50 myocardial fibers were measured at the level of nuclei while omitting longitudinally or obliquely sectioned cells as described earlier.[18] Magnitudes of perivascular fibrosis or collagen volume fraction in the interstitial space of myocardial fibers were also determined as described earlier.[18]

Gene expression

Gene expressions of transforming growth factor (TGF)-β1, type 1 collagen and ACE in the LV were measured by real-time quantitative reverse transcription-PCR (ABI Prism 7700 Sequence Detector, Applied Biosystems, Foster City, CA, USA).[18,24] Total RNA Isolation Reagent (Invitrogen, Carlsbad, CA, USA) was used to extract 1 μg of total RNA, which then underwent reverse transcription by means of SuperScript reverse transcriptase (Invitrogen) into cDNA. cDNA was then amplified with oligonucleotide forward and reverse primers and with probes labeled with 6-carboxy-fluorescencein as reporter fluorescence and 6-carboxy-tetramethyl-rhodamine as quencher fluorescence. The oligonucleotide sequences are detailed in earlier reports.[18,24,25] The PCR products were of the expected molecular sizes and the gene expression levels were standardized to those of 18S rRNA.

Cell culture

Cardiac fibroblasts were isolated from 1- to 3-day-old neonatal Wistar rats as described earlier.[18] The cells were grown on culture plates with Dulbecco's modified Eagle's medium containing 10% fetal bovine serum, 10 μg ml^{-1}

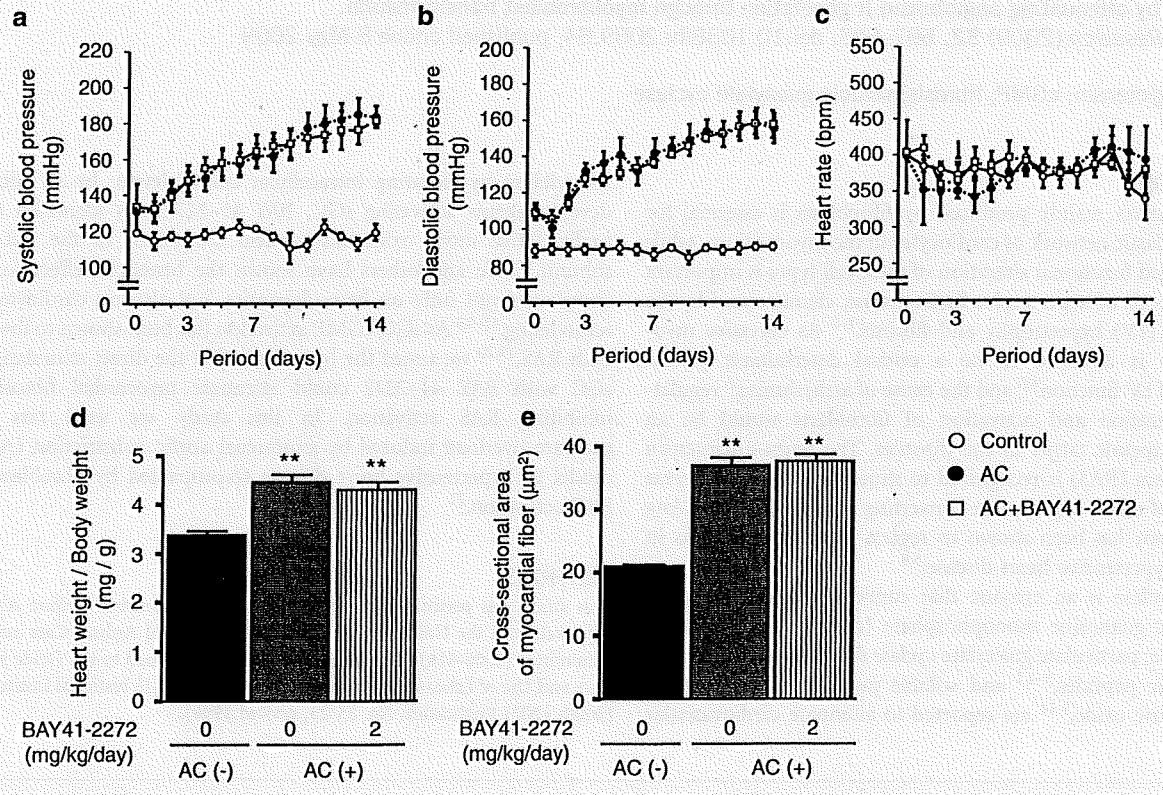

Figure 1 (**a–c**) Effects of BAY 41–2272 on systolic (**a**) and diastolic (**b**) blood pressure levels and heart rate (**c**). (**d** and **e**) Effects of BAY41–2272 on heart weight/body weight (**d**) and cross-sectional area of myocardial fibers (**e**). Open circle (○), closed circle (●) and open square (□) indicate the control, aortic constriction (AC) and AC plus BAY 41–2272 treatment, respectively. $^{**}P<0.01$, compared with the controls. Values are shown as the means ± s.e.m. of four rats (for blood pressure and heart rate) and of 11–21 rats (for heart weight, cross-sectional area of myocardial fibers) in the respective group.

insulin, 5 μg ml^{-1} transferrin and 7 ng ml^{-1} sodium selenite at 37 °C in a 95% air/5% CO_2 humidified atmosphere. After achieving confluence, they were further incubated in serum-free Dulbecco's modified Eagle's medium containing the same additives for 48 h. The cells were then cultured with BAY 41–2272 (10^{-6} and 10^{-5} mol l^{-1}) or non-hydrolysable cGMP analog 8-bromo cGMP (10^{-4} and 10^{-3} mol l^{-1}) (Calbiochem, San Diego, CA, USA) dissolved in dimethyl sulfoxide for a further 24 h. The same volume of dimethyl sulfoxide was added to the control culture medium, and the final concentration of dimethyl sulfoxide did not exceed 0.1% in the culture medium. Thereafter, the cells were collected, and total protein was extracted for western blot as described earlier.[24] In addition, they were extracted to measure ACE activity as described below. The extracted proteins were stored at −80 °C until use.

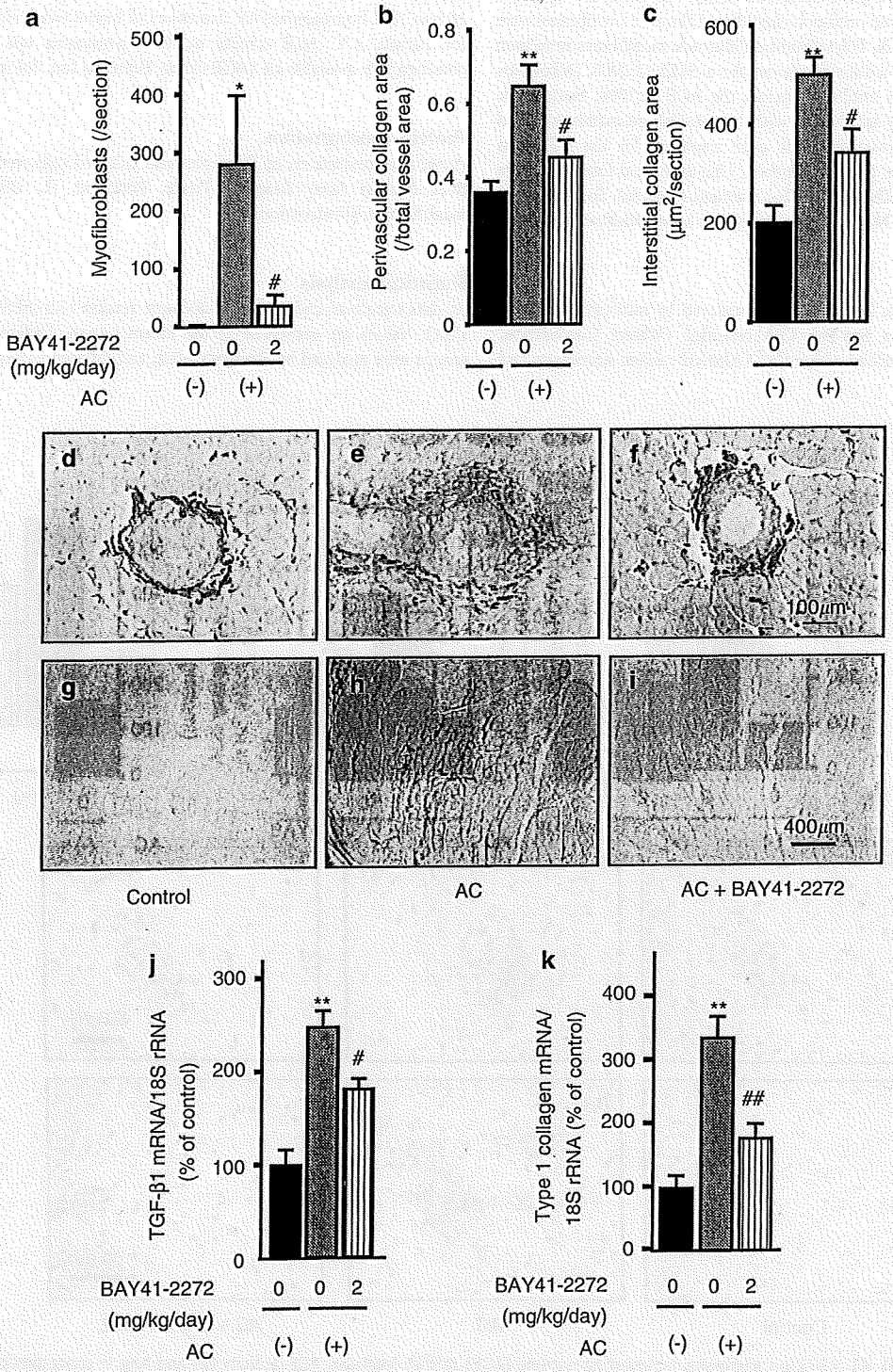

Figure 2 (a–c) Effects of BAY 41–2272 on the number of myofibroblasts determined by positive staining for α-SMA (**a**), picrosirius red-positive areas in adventitia of intramyocardial coronary arteries (**b**) and myocardial interstitium (**c**). The panels are representative images of picrosirius red staining in the control (**d** and **g**) and aortic constriction (AC) rats without (**e** and **h**) or with (**f** and **i**) BAY 41–2272 treatment. (**j** and **k**) Effects of BAY 41–2272 on gene expressions for transforming growth factor-β1 (**j**) and type 1 collagen (**k**). Values are shown as the means ± s.e.m. of 9–19 samples in the respective group. $^{*}P<0.05$, $^{**}P<0.01$, compared with the controls; $^{\#}P<0.05$, $^{\#\#}P<0.01$, compared with AC rats without BAY 41–2272 treatment.

Cardiac myocytes were also isolated from 1- to 3-day-old neonatal Wistar rats as described earlier.[26] After culturing the cells under the serum-free Dulbecco's modified Eagle's medium containing 10 μg ml^{-1} insulin, 5 μg ml^{-1} transferrin and 7 ng ml^{-1} sodium selenite for 48 h, BAY 41–2272 (10^{-6} and 10^{-5} mol l^{-1}) was then added to the medium to examine the intracellular cGMP elevation.

Western blot

Denatured total protein obtained from cultured cardiac fibroblasts was subjected to SDS-polyacrylamide gel as described earlier.[12] In brief, the separated proteins electrically transferred onto polyvinylidine difluoride membranes were incubated with 5% skim milk. Polyvinylidine difluoride membranes were then incubated with monoclonal antibody against the α-SMA (1:2000, DakoCytomation) or with polyclonal antibody against the ACE (1:1000, Santa Cruz Biotechnology), followed by incubation with horseradish peroxidase-coupled second antibody. Immunoreactive bands were visualized by the ECL Plus detection kit (GE Healthcare, Buckinghamshire, UK) and band intensities were analyzed densitometrically (Chemi Doc Documentation System, Bio-Rad, Hercules, CA, USA). Coomassie blue staining was used as a protein-loading control.

Radioimmunoassay

Angiotensin II concentration in the LV was measured by radioimmunoassay, following extraction with a Sep-Pak C18 cartridge (Waters Corporation, Milford, MA, USA), as described earlier.[18,27] Cultured cardiac fibroblasts and myocytes treated with or without BAY 41–2272 for 10 min were immediately collected, and the cGMP content was determined using a radioimmunoassay kit (YAMASA Cyclic GMP Assay Kit, Choshi, Japan).[18]

ACE activity

The LV tissues in the respective groups were homogenized in phosphate-buffered saline. Cultured cardiac fibroblasts treated with or without BAY 41–2272 or 8-bromo cGMP for 24 h were collected in 1.8% Triton-X containing phosphate-buffered saline, and were lysed by freezing-thawing three times every 10 min. The homogenized LV tissues or cell lysates were centrifuged at 10 000 *g* for 10 min, 4 °C ACE activity in the supernatants was measured with a commercially available kit (ACE Color, Fujirebio Inc. Tokyo, Japan).

Protein concentration

Protein concentrations of LV tissues and cultured cells were determined with BCA Protein Assay Reagent (Pierce, Rockland, IL, USA), following the manufacturer's instructions.

Statistical analysis

All data were analyzed with SPSS software version 11.0 (SPSS Inc., Chicago, IL, USA). Values are expressed as the means ± s.e.m. Differences between two groups were analyzed by Student's *t*-test, and differences between three groups

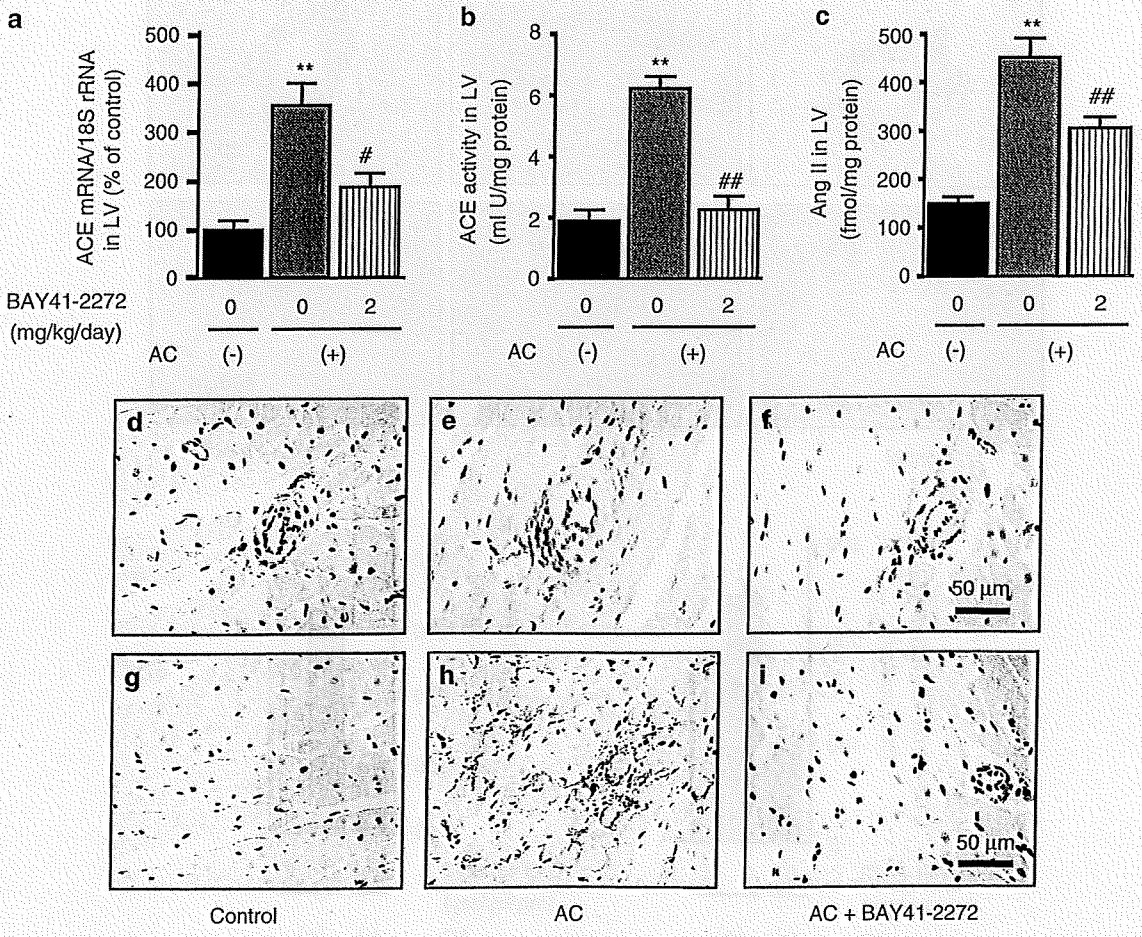

Figure 3 (a–c) Effects of BAY 41–2272 on angiotensin-converting enzyme (ACE) mRNA level (a), ACE activity (b) and Ang II concentration (c) in the left ventricle (LV). The panels are representative images of ACE immunoreactivity in the control (d and g) and aortic constriction (AC) rats without (e and h) or with (f and i) BAY 41–2272 treatment. Bar: 50 μm. Values are shown as the means ± s.e.m. of 11–16 in the respective group. $^{**}P<0.01$, compared with the controls; $^{\#}P<0.05$, $^{\#\#}P<0.01$, compared with AC rats without BAY 41–2272.

were assessed using one-way analysis of variance followed by Scheffé's test, and statistical significance was accepted at $P<0.05$. In western blot analysis, standard curves were made by serial dilution of samples, and bands on gels were quantified based on the optical density.

RESULTS

Hemodynamics, heart weight and cardiocyte size

Figures 1a–c show the blood pressure and heart rate in the controls and AC rats with or without BAY 41–2272 treatment. AC progressively raised systolic and diastolic blood pressure levels; however, BAY 41–2272 had no effect on the AC-induced elevation of blood pressure. Heart rate was unchanged in the respective groups. As shown in Figures 1d and e, AC significantly ($P<0.01$) increased the ratio of heart weight to body weight (HW/BW) and the cross-sectional area of myocardial fibers, compared with the controls; however, BAY 41–2272 did not affect the AC-induced increase in HW/BW and cardiocyte size.

Myofibroblasts and collagen deposition

Figures 2a–c show that AC increased the number of myofibroblasts and collagen depositions in the perivascular and the interstitial areas of LV, but BAY 41–2272 administration significantly ($P<0.05$) decreased them by 88, 30 and 46%, respectively. Representative collagen deposition in the respective groups are shown in Figures 2d–i. As shown in Figures 2j and k, BAY 41–2272 administration significantly ($P<0.05$) attenuated the AC-induced elevation of gene expressions of TGF-β1 and type 1 collagen.

Ang II synthesis

Figure 3a and b show that AC significantly ($P<0.01$) increased the gene expression and activity of ACE in LV, but BAY 41–2272 significantly ($P<0.01$) reduced them by 47 and 64%, respectively. Figure 3c shows that BAY 41–2272 administration significantly ($P<0.01$) attenuated the AC-induced increase of Ang II concentration in LV by 36%. As shown in Figures 3d–i, ACE immunoreactivity

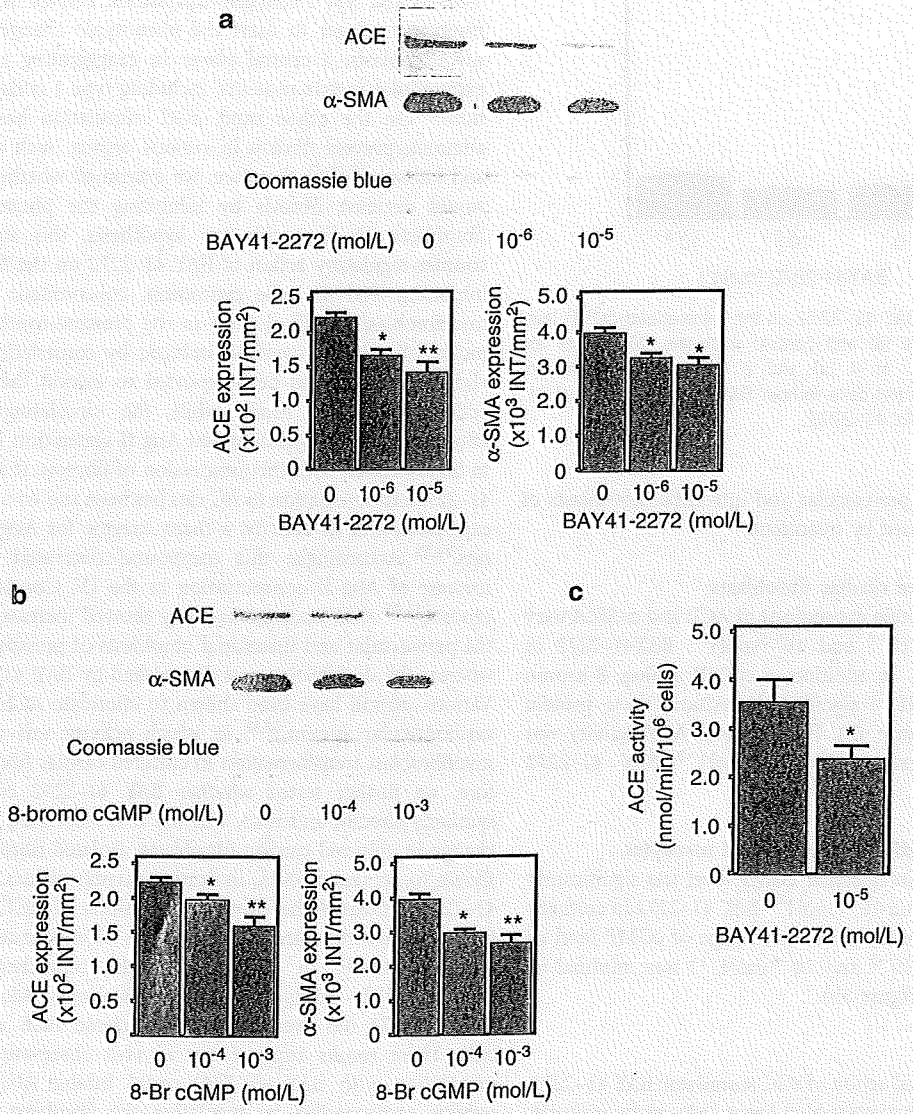

Figure 4 (a and b) Effects of BAY 41–2272 (a) and cGMP analog 8-bromo cGMP (b) on the protein expressions of angiotensin-converting enzyme (ACE) and α-smooth muscle actin (α-SMA) in cultured cardiac fibroblasts. (c) Effect of BAY 41–2272 on ACE activity in cell lysates. The panels show representative images of western blotting, and values are shown as the means ± s.e.m. of 4–6 (a and b), 9 and 11 (c) samples examined. *$P<0.05$, **$P<0.01$, compared with control cells without either BAY 41–2272 or 8-bromo cGMP. Coomassie blue was used as the protein loading control.

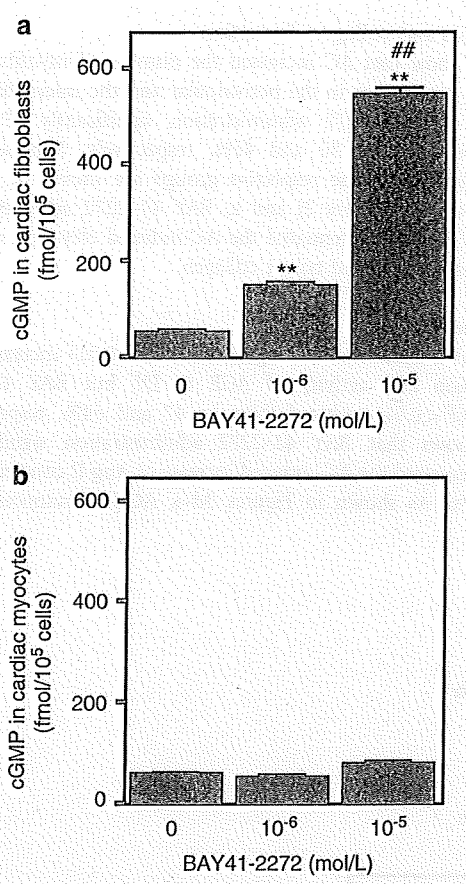

Figure 5 (**a** and **b**) Effect of BAY 41–2272 on the intracellular cGMP level in cultured cardiac fibroblasts (**a**) and cardiac myocytes (**b**). Values are shown as the means ± s.e.m. of 4 (**a**) and 8 (**b**) samples examined. $^{**}P<0.01$, compared with control cells without BAY 41–2272, $^{\#\#}P<0.01$, compared with 10^{-6} mol l^{-1} BAY 41–2272.

increased to localize in the perivascular and interstitial fibroblasts of AC rats, while it was decreased by treatment.

ACE and α-SMA in cultured cardiac fibroblasts

Figure 4a shows that the protein expressions of ACE and α-SMA were significantly decreased by 10^{-6} and 10^{-5} mol l^{-1} BAY41–2272 in cultured cardiac fibroblasts. In addition, a cGMP analog, 8-bromo cGMP (10^{-4} and 10^{-3} mol l^{-1}) significantly reduced these protein expressions in the cells (Figure 4b). Furthermore, ACE activity was significantly ($P<0.05$) decreased by 10^{-5} mol l^{-1} BAY 41–2272 (Figure 4c).

cGMP level in cultured cardiac fibroblasts and myocytes

As shown in Figure 5a, the intracellular cGMP level was significantly ($P<0.01$) elevated by 10^{-5} and 10^{-6} mol l^{-1} BAY 41–2272 in cultured cardiac fibroblasts. On the other hand, the change of cGMP level in response to BAY 41–2272 (10^{-5} and 10^{-6} mol l^{-1}) was minimal in cultured cardiac myocytes (Figure 5b).

DISCUSSION

This study shows the beneficial action of sGC stimulator BAY 41–2272 on attenuating fibrosis in a hypertrophied heart induced by pressure overload, independently of blood pressure. In addition, the inhibition of myofibroblast transformation and RAS activation appear be involved in this mechanism.

We have earlier reported that the depressor dose of sGC stimulation with BAY 41–2272 was effective to decrease cardiocyte hypertrophy and fibrosis, but the sub-depressor dose exhibited to decrease fibrosis without reducing cardiocyte hypertrophy in the Ang II-induced hypertensive model.[18] This study was consistent to show that the sub-depressor dose of this compound decreased the fibrosis without altering cardiocyte hypertrophy defined by HW/BW and cross-sectional area of myocardial fiber in the model of pressure overload. Although precise mechanisms by which the sub-depressor dose of sGC stimulation facilitates to decrease fibrosis remain to be elucidated, we might speculate the discrepancy between fibrosis and heart weight in response to the sGC stimulation by the following two reasons: (1) mechanical load is a major contributor to cardiocyte hypertrophy,[7] and therefore the sub-depressor dose BAY 41–2272 was insufficient to influence the cardiocyte hypertrophy induced by pressure-overload; (2) *in vitro* experiment suggests that cardiac fibroblasts appear to be more feasible to exert cGMP elevation than cardiac myocytes by the compound. Using a sub-depressor dose of BAY 41–2272, the attenuation of fibrosis by this compound was associated with the reduction of TGF-β1 and type 1 collagen expressions. TGF-β1 is reported to be an important trigger to exert the phenotypic change of fibroblasts to myofibroblasts, a central player in exaggerating the production of extracellular matrix proteins, including type 1 collagen and fibronection.[28] On the other hand, sGC stimulation has been shown to attenuate/prevent fibrosis in various organs, such as the lungs, liver and kidneys;[20,29–31] therefore, we examined whether this compound would decrease fibrosis by inhibiting the phenotypic change in fibroblasts. In line with our hypothesis, this study suggests the counter-regulatory action of BAY 41–2272 on the fibrotic process by inhibiting TGF-β1 gene expression, concomitant with attenuating myofibroblast transformation in the pressure-overloaded heart. The model of pressure overload induced by constricting the suprarenal abdominal aorta has been reported to exhibit the substantial RAS activation in the heart, while the circulating RAS was less affected,[21,22,32,33] suggesting that Ang II generation in the LV is likely to be associated with the progression of fibrosis. It is noted that BAY 41–2272 administration to AC rats has been shown to lower ACE gene expression and its activity, a main enzyme for Ang II generation in rats.[34,35] Accordingly, this compound decreased the AC-induced increase of Ang II concentration in the LV. Consistent with earlier reports,[34,35] ACE immunoreactivity showed increased distribution in the perivascular and interstitial fibroblasts of pressure-overloaded LV, whereas the distribution was diminished by BAY 41–2272 treatment. Various stimuli have been shown to stimulate ACE synthesis in the cardiovascular system,[36,37] in which activity was increased during myofibroblast transformation in cultured cardiac fibroblasts.[38] Therefore, we further tested whether BAY 41–2272 could affect ACE synthesis directly, and if so, whether it is associated with phenotypic change in cultured cardiac fibroblasts. Isolated fibroblasts have been shown to express α-SMA, indicating myofibroblasts. As shown, BAY 41–2272 decreased the protein expressions of ACE and α-SMA in these cells, accompanied by intracellular cGMP elevation. In addition, 8-bromo cGMP, an analog of cGMP, mimicked the effect of BAY 41–2272, inhibiting these expressions. More importantly, BAY 41–2272 has been shown to decrease ACE activity in these cells. These results support our *in vivo* observations, which sGC stimulation with BAY 41–2272 could inhibit ACE synthesis and activity, accompanied by regulating the fibroblast phenotype. We have earlier reported that BAY 41–2272 was capable of inhibiting cardiac fibroblast proliferation under Ang II stimulation.[18] Taken together, we propose that pharmacological intervention with the orally

effective sGC stimulator BAY 41–2272 points to an antifibrotic action, in which the inhibition of myofibroblasts transformation and Ang II synthesis might induce specific benefits against the development of hypertensive heart disease.

In summary, sGC stimulation with BAY 41–2272 attenuated cardiac fibrosis independently of blood pressure, and the inhibition of myofibroblast transformation and Ang II synthesis appear to be the potential mechanisms involved. Thus, our present study supports the sGC-cGMP-dependent beneficial action against adverse cardiovascular remodeling associated with hypertension. Further studies are warranted to clarify the long-term benefit and safety of this compound for future's clinical practice.

CONFLICT OF INTEREST

Toshihiro Tsuruda received a research grant from Bayer HealthCare. BAY 41–2272 was synthesized at Bayer HealthCare as a research tool but not for use in humans.

ACKNOWLEDGEMENTS

We thank Ms Ritsuko Sotomura for technical assistance. This study was supported by Grants-in-aid for Scientific Research (C) (20590830) from the Ministry of Education, Culture, Sports, Science, and Technology, Japan and from Bayer HealthCare.

1 Levy D, Larson MG, Vasan RS, Kannel WB, Ho KK. The progression from hypertension to congestive heart failure. *JAMA* 1996; **275**: 1557–1562.
2 Kai H, Kuwahara F, Tokuda K, Imaizumi T. Diastolic dysfunction in hypertensive hearts: roles of perivascular inflammation and reactive myocardial fibrosis. *Hypertens Res* 2005; **28**: 483–490.
3 Diamond JA, Phillips RA. Hypertensive heart disease. *Hypertens Res* 2005; **28**: 191–202.
4 Müller-Brunotte R, Kahan T, López B, Edner M, González A, Díez J, Malmqvist K. Myocardial fibrosis and diastolic dysfunction in patients with hypertension: results from the Swedish Irbesartan Left Ventricular Hypertrophy Investigation versus Atenolol (SILVHIA). *J Hypertens* 2007; **25**: 1958–1966.
5 Díez J, Querejeta R, López B, González A, Larman M, Martínez Ubago JL. Losartan-dependent regression of myocardial fibrosis is associated with reduction of left ventricular chamber stiffness in hypertensive patients. *Circulation* 2002; **105**: 2512–2517.
6 McLenachan JM, Dargie HJ. Ventricular arrhythmias in hypertensive left ventricular hypertrophy. Relationship to coronary artery disease, left ventricular dysfunction, and myocardial fibrosis. *Am J Hypertens* 1990; **3**: 735–740.
7 Weber KT. Fibrosis and hypertensive heart disease. *Curr Opin Cardiol* 2000; **15**: 264–272.
8 Brilla CG, Funck RC, Rupp H. Lisinopril-mediated regression of myocardial fibrosis in patients with hypertensive heart disease. *Circulation* 2000; **102**: 1388–1393.
9 Calderone A, Thaik CM, Takahashi N, Chang DL, Colucci WS. Nitric oxide, atrial natriuretic peptide, and cyclic GMP inhibit the growth-promoting effects of norepinephrine in cardiac myocytes and fibroblast. *J Clin Invest* 1998; **101**: 812–818.
10 Mori T, Chen YF, Feng JA, Hayashi T, Oparil S, Perry GJ. Volume overload results in exaggerated cardiac hypertrophy in the atrial natriuretic peptide knockout mouse. *Cardiovasc Res* 2004; **61**: 771–779.
11 Cao L, Gardner DG. Natriuretic peptides inhibit DNA synthesis in cardiac fibroblasts. *Hypertension* 1995; **25**: 227–234.
12 Tsuruda T, Boerrigter G, Huntley BK, Noser JA, Cataliotti A, Costello-Boerrigter LC, Chen HH, Burnett Jr JC. Brain natriuretic peptide is produced in cardiac fibroblasts and induces matrix metalloproteinases. *Circ Res* 2002; **91**: 1127–1134.
13 Tamura N, Ogawa Y, Chusho H, Nakamura K, Nakao K, Suda M, Kasahara M, Hashimoto R, Katsuura G, Mukoyama M, Itoh H, Saito Y, Tanaka I, Otani H, Katsuki M. Cardiac fibrosis in mice lacking brain natriuretic peptide. *Proc Natl Acad Sci USA* 2000; **97**: 4239–4244.
14 Kim NN, Villegas S, Summerour SR, Villarreal FJ. Regulation of cardiac fibroblast extracellular matrix production by bradykinin and nitric oxide. *J Mol Cell Cardiol* 1999; **31**: 457–466.
15 Stasch JP, Becker EM, Alonso-Alija C, Apeler H, Denbowsky K, Feurer A, Gerzer R, Minuth T, Perzborn E, Pleiß U, Schröder H, Schroeder W, Stahl E, Steinke W, Straub A, Schramm M. NO-independent regulatory site on soluble guanylate cyclase. *Nature* 2001; **410**: 212–215.
16 Boerrigter G, Costello-Boerrigter LC, Cataliotti A, Tsuruda T, Harty GJ, Lapp H, Stasch JP, Burnett Jr JC. Cardiorenal and humoral properties of a novel direct soluble guanylate cyclase stimulator BAY41–2272 in experimental congestive heart failure. *Circulation* 2003; **107**: 686–689.
17 Evgenov OV, Ichinose F, Evgenov NV, Gnoth MJ, Falkowski GE, Chang Y, Bloch KD, Zapol WM. Soluble guanylate cyclase activator reverses acute pulmonary hypertension and augments the pulmonary vasodilator response to inhaled nitric oxide in awake lambs. *Circulation* 2004; **110**: 2253–2259.
18 Masuyama H, Tsuruda T, Kato J, Imamura T, Asada Y, Stasch JP, Kitamura K, Eto T. Soluble guanylate cyclase stimulation on cardiovascular remodeling in angiotensin II-induced hypertensive rats. *Hypertension* 2006; **48**: 972–978.
19 Yan C, Kim D, Aizawa T, Berk BC. Functional interplay between angiotensin II and nitric oxide: cyclic GMP as a key mediator. *Arterioscler Thromb Vasc Biol* 2003; **23**: 26–36.
20 Dunkern TR, Feurstein D, Rossi GA, Sabatini F, Hatzelmann A. Inhibition of TGF-β induced lung fibroblast to myofibroblast conversion by phosphodiesterase inhibiting drugs and activators of soluble guanylyl cyclase. *Eur J Pharmacol* 2007; **572**: 12–22.
21 Kuwahara F, Kai H, Tokuda K, Kai M, Takeshita A, Egashira K, Imaizumi T. Transforming growth factor-β function blocking prevents myocardial fibrosis and diastolic dysfunction in pressure-overloaded rats. *Circulation* 2002; **106**: 130–135.
22 Hirano S, Imamura T, Onitsuka H, Matsuo T, Kitamura K, Koiwaya Y, Eto T. Rapid increase in cardiac adrenomedullin gene expression caused by acute pressure overload: effect of the renin-angiotensin system on gene expression. *Circ J* 2002; **66**: 397–402.
23 Tonkiss J, Trzcivska M, Galler JR, Ruiz-Opazo N, Herrera VLM. Prenatal malnutrition-induced changes in blood pressure. Dissociation of stress and nonstress responses using radiotelemetry. *Hypertension* 1998; **32**: 108–114.
24 Tsuruda T, Kato J, Hatakeyama K, Masuyama H, Cao YN, Imamura T, Kitamura K, Asada Y, Eto T. Antifibrotic effect of adrenomedullin on coronary adventitia in angiotensin II-induced hypertensive rats. *Cardiovasc Res* 2005; **65**: 921–929.
25 Naito Y, Tsujino T, Fujioka Y, Ohyanagi M, Iwasaki T. Augmented diurnal variations of the cardiac renin-angiotensin system in hypertensive rats. *Hypertension* 2002; **40**: 827–833.
26 Tsuruda T, Kato J, Kitamura K, Kuwasako K, Imamura T, Koiwaya Y, Tsuji T, Kangawa K, Eto T. Adrenomedullin: a possible autocrine or paracrine inhibitor of hypertrophy of cardiomyocytes. *Hypertension* 1998; **31**: 505–510.
27 Nagata S, Kato J, Sasaki K, Minamino N, Eto T, Kitamura K. Isolation and identification of proangiotensin-12, a possible component of the renin-angiotensin system. *Biochem Biophys Res Commun* 2006; **350**: 1026–1031.
28 Powell DW, Mifflin RC, Valentich JD, Crowe SE, Saada JI, West AB. Myofibroblasts. I. Paracrine cells important in health and disease. *Am J Physiol* 1999; **277**: C1–C9.
29 Wang Y, Krämer S, Loof T, Martini S, Kron S, Kawachi H, Shimizu F, Neumayer HH, Peters H. Enhancing cGMP in experimental progressive renal fibrosis: soluble guanylate cyclase stimulation vs phosphodiesterase inhibition. *Am J Physiol Renal Physiol* 2006; **290**: F167–F176.
30 Kalk P, Godes M, Relle K, Rothkegel C, Hucke A, Stasch JP, Hocher B. NO-independent activation of soluble guanylate cyclase prevents disease progression in rats with 5/6 nephrectomy. *Br J Pharmacol* 2006; **148**: 853–859.
31 Knorr A, Hirth-Dietrich C, Alonso-Alija C, Härter M, Hahn M, Keim Y, Wunder F, Stasch JP. Nitric oxide-independent activation of soluble guanylate cyclase by BAY 60–2770 in experimental liver fibrosis. *Arzneimittelforschung* 2008; **58**: 71–80.
32 Tokuda K, Kai H, Kuwahara F, Yasukawa H, Tahara N, Kudo H, Takemiya K, Koga M, Yamamoto T, Imaizumi T. Pressure-independent effects of angiotensin II on hypertensive myocardial fibrosis. *Hypertension* 2004; **43**: 499–503.
33 Kobayashi S, Yano M, Kohno M, Obayashi M, Hisamatsu Y, Ryoke T, Ohkusa T, Yamakawa K, Matsuzaki M. Influence of aortic impedance on the development of pressure-overload left ventricular hypertrophy in rats. *Circulation* 1996; **94**: 3362–3368.
34 Kurosawa Y, Katoh M, Doi H, Narita H. Tissue angiotensin-converting enzyme activity plays an important role in pressure overload-induced cardiac fibrosis in rats. *J Cardiovasc Pharmacol* 2002; **39**: 600–609.
35 de Lannoy LM, Schuijt MP, Saxena PR, Schalekamp MA, Danser AH. Angiotensin converting enzyme is the main contributor to angiotensin I-II conversion in the interstitium of the isolated perfused rat heart. *J Hypertens* 2001; **19**: 959–965.
36 Barreto-Chaves ML, Anéas I, Krieger JE. Glucocorticoid regulation of angiotensin-converting enzyme in primary culture of adult cardiac fibroblasts. *Am J Physiol Regul Integr Comp Physiol* 2001; **280**: R25–R32.
37 Saijonmaa O, Nyman T, Kosonen R, Fyhrquist F. Upregulation of angiotensin-converting enzyme by vascular endothelial growth factor. *Am J Physiol Heart Circ Physiol* 2001; **280**: H885–H891.
38 Petrov VV, Fagard RH, Lijnen PJ. Transforming growth factor-β1 induces angiotensin-converting enzyme synthesis in rat cardiac fibroblasts during their differentiation to myofibroblasts. *J Renin Angiotensin Aldosterone Syst* 2000; **1**: 342–352.

Regulatory Peptides 158 (2009) 127–131

Contents lists available at ScienceDirect

Regulatory Peptides

journal homepage: www.elsevier.com/locate/regpep

Increased plasma levels of the mature and intermediate forms of adrenomedullin in obesity

Ikuo Nomura [a], Johji Kato [b,*], Mariko Tokashiki [a], Kazuo Kitamura [a]

[a] Department of Internal Medicine, Circulatory and Body Fluid Regulation, Faculty of Medicine, University of Miyazaki, Kiyotake, Miyazaki 889-1692, Japan
[b] Frontier Science Research Center, University of Miyazaki, 5200 Kihara, Kiyotake, Miyazaki 889-1692, Japan

ARTICLE INFO

Article history:
Received 23 April 2009
Received in revised form 20 June 2009
Accepted 16 August 2009
Available online 23 August 2009

Keywords:
Body mass index
Insulin sensitivity
Metabolic disorder

ABSTRACT

Adrenomedullin (AM) is a cardiovascular protective peptide produced in various organs and tissues including adipose tissue. In the present study, we measured the plasma AM levels of subjects with or without obesity by two assay methods to separately evaluate the biologically active AM–NH_2 and the intermediate form of AM–glycine (AM–Gly). We measured the total AM and AM–NH_2 levels of plasma in 52 obese and 172 non-obese residents of a Japanese community, who received regular health check-ups and had no overt cardiovascular disease. AM–Gly values were obtained by subtracting AM–NH_2 levels from those of total AM. Both the AM–NH_2 and AM–Gly levels of the subjects with obesity were higher than those without obesity, and significant relationships were noted between body mass index (BMI) and the plasma levels of the two molecular forms of AM in a simple regression analysis. Moreover, the significant factors identified by multivariate analyses were BMI and serum triglyceride for AM–NH_2 and diastolic blood pressure, insulin, high-density lipoprotein-cholesterol, and plasma renin activity for AM–Gly. These results suggest active roles for the two molecular forms of AM in metabolic disorders associated with obesity in subjects without overt cardiovascular disease.

1. Introduction

Consisting of 52 amino-acid residues, adrenomedullin (AM) is a biologically active peptide that exerts a wide range of actions including vasodilatation, improvement of vascular endothelial function, inhibition of cardiovascular remodeling, modulation of adipogenesis, and alleviation of insulin resistance [1–7]. Although it was initially isolated from pheochromocytoma tissue, the AM peptide is produced in various organs such as the adrenal medulla, heart, blood vessels, and adipose tissue [1–9]. AM also circulates in human blood, and plasma AM levels were found to be elevated in patients with hypertension, obesity, heart failure, acute myocardial infarction, and atherosclerotic vascular diseases [2–4,10–13]. Based on its biological actions, AM is assumed to participate in mechanisms that act against the development or progression of metabolic or cardiovascular diseases. In the biosynthesis of AM peptide, the intermediate form AM–glycine (AM–Gly) is processed from the AM precursor proAM, a 126 amino-acid peptide, and then the biologically active mature form of AM–NH_2 is produced by the action of amidation enzymes [2–4]. We previously reported that AM in the human blood consists of two molecular forms, the mature and intermediate AM peptides [14]. There have been a number of reports on AM measurement in human plasma; however, the assay methods used in most of these studies were unable to measure the mature and intermediate AM levels separately [2–4,14]. In the present study, we measured plasma AM levels with two types of immunoreactive radiometric assays (IRMA) to detect AM–NH_2 and AM–Gly in non-obese and obese residents of a Japanese community without overt cardiovascular disease. We then compared these AM levels with other clinical parameters, to study the pathophysiological role of AM in obesity-related metabolic disorders.

2. Materials and methods

2.1. Study subjects and protocol

Local residents of the Kiyotake area, Miyazaki, Japan, who underwent an annual regular health check-up in 2007 were examined for this study (81 males and 143 females; 60.8 ± 9.8 years, mean ± SD). Upon visiting the community center of Kiyotake town, the medical history of the subjects was taken by nurses and confirmed by physicians. The subjects enrolled were determined to have no overt cardiovascular diseases such as ischemic heart disease, congestive heart failure, or stroke from their medical history and physical examination, and those given glucose-lowering agents for diabetes mellitus were excluded from this study to allow the precise evaluation of insulin-sensitivity. Obesity was defined as a body mass index (BMI) of 25 Kg/m^2 or higher, according to the criteria of the Japan Society for the Study of Obesity [15]. Blood pressure was measured with an oscillometric automatic device (BP-103ill, Colin, Japan) in a sitting

* Corresponding author. Tel.: +81 985 85 9718; fax: +81 985 85 6596.
E-mail address: jkjpn@med.miyazaki-u.ac.jp (J. Kato).

0167-0115/$ – see front matter © 2009 Elsevier B.V. All rights reserved.
doi:10.1016/j.regpep.2009.08.003

Table 1
The basal profile of the subjects examined in this study.

	Non-obese	Obese
Male/female (*n*)	57/115	24/28
Age (year)	60.5±9.7	61.5±10.3
SBP (mmHg)	123±18	134±17**
DBP (mmHg)	74±11	79±10**
BMI (kg/m^2)	21.4±2.0	27.5±3.3**
Serum creatinine (mg/dl)	0.71±0.14	0.76±0.19

SBP and DBP: systolic and diastolic blood pressure; BMI: body mass index; mean±SD; **$P<0.01$.

Table 2
Metabolic and humoral factors.

	Non-obese	Obese
Fasting blood glucose (mg/dl)	96±16	106±26**
Insulin (μIU/ml)	4.3±2.0	8.9±5.4**
HOMA index	1.04±0.52	2.47±2.40**
Cholesterol (mg/dl)	211±32	213±32
HDL-cholesterol (mg/dl)	64±13	56±13**
Triglyceride (mg/dl)	97±54	123±86**
Plasma renin activity (ng/ml/h)	0.87±0.64	0.88±0.54
Plasma aldosterone (pg/ml)	87±45	92±40

HOMA: homeostasis model assessment; HDL: high-density lipoprotein; mean±SD; **$P<0.01$.

position by experienced nurses, and then blood was drawn from an antecubital vein after overnight fasting. To measure the total and mature AM levels in plasma, blood was collected in tubes with 1.0 mg/mL

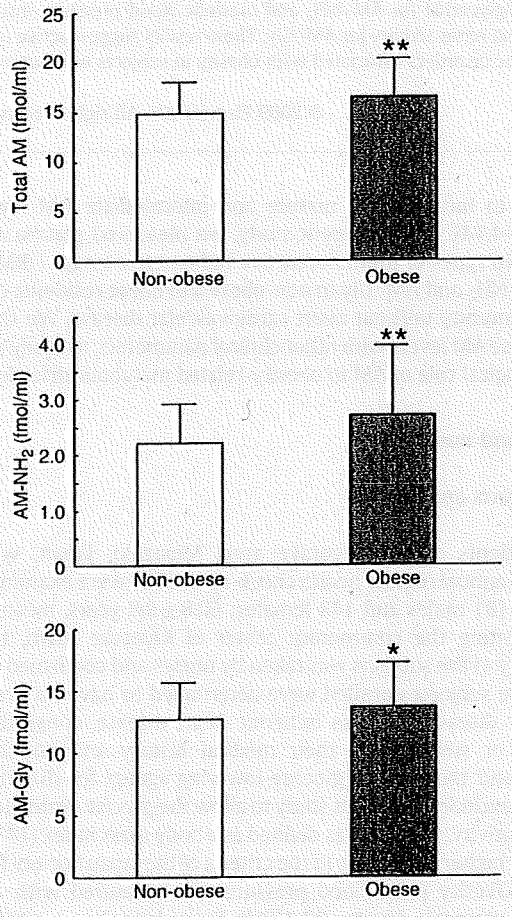

Fig. 1. Plasma levels of total AM, AM-NH_2, and AM-Gly in non-obese and obese subjects. The data are shown as means±SD. *$P<0.05$, **$P<0.01$, vs. non-obese subjects.

Table 3
Coefficients of correlation obtained by simple regression analysis.

	AM-NH_2	AM-Gly
Basal parameters		
Age	0.142*	n.s.
BMI	0.222**	0.211**
SBP	0.152*	0.259**
DBP	0.149*	0.296**
Serum creatinine	n.s.	0.181**
Metabolic or humoral parameters		
Insulin	n.s.	0.313**
HOMA index	n.s.	0.293**
HDL-cholesterol	n.s.	−0.266**
Triglycerides	0.198**	0.273**
Plasma renin activity	n.s.	0.199**

The abbreviations are listed in Tables 1 and 2. *$P<0.05$, **$P<0.01$, n.s. = not significant.

of EDTA-2Na and 500 kallikrein inhibitory units (KIU)/mL of aprotinin. Plasma was obtained by centrifugation at 3000 rpm for 10 min at 4 °C and stored at −40 °C until the assay.

This study was approved by the Review Committee for Cooperative and Commissioned Research and the Ethics Committee of the University of Miyazaki Faculty of Medicine. All subjects examined gave their written informed consent before participating in this study.

2.2. Assay procedures

Total and mature AM levels were measured by AM RIA and AM mature RIA (Shionogi Pharmaceutical Co., Ltd., Osaka, Japan), respectively [16,17], and values for the intermediate form AM-Gly were obtained by subtracting the plasma levels of AM-NH_2 from those of total AM. The details of these assays are described in the original reports by Ohta et al. and those of others [7,16,17]. Plasma

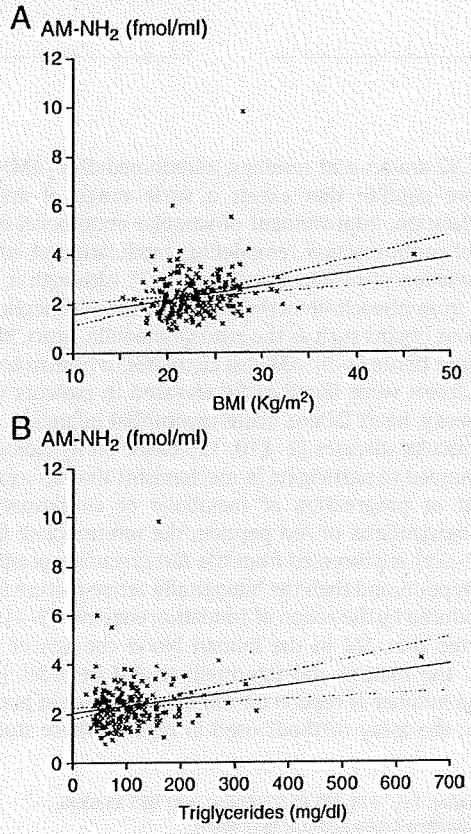

Fig. 2. Relationships between the AM-NH_2 and BMI (A) or serum triglyceride level (B). Regression lines and 95% confidence limits are shown on each graph.